Title
Single Axis Optical Focus Mechanism for Telescope on Small Satellite

Author
Karburn, Jordan

Publication Date
2021

Peer reviewed|Thesis/dissertation

Single Axis Optical Focus Mechanism for Telescope on Small Satellite

By

JORDAN KARBURN

THESIS

Submitted in partial satisfaction of the requirements for the degree of

MASTER OF SCIENCE

in

Electrical and Computer Engineering

in the

OFFICE OF GRADUATE STUDIES

of the

UNIVERSITY OF CALIFORNIA

DAVIS

Approved:

Andre Knoesen

William Putnam

Pete Supsinskas

Committee in Charge

2021

External Audience (Unlimited), LLNL-TH-819121.
Prepared by LLNL under Contract DE-AC52-07NA27344.

Abstract

The following research proposes an approach for an on-orbit single axis focus control mechanism in optical telescopes on small satellites. This solution addresses the need in the aerospace industry for maintaining orbital optical performance, in various extreme environmental conditions, while adhering to the severe size, weight, and power constraints of small satellites. A heavy emphasis in this effort is on the Systems Engineering approach to design, build and test. Considerable time is spent identifying the key stakeholders, categorizing design constraints, developing system requirements, conducting design trades, and comparing potential solutions. The chosen design is an electro-mechanical mechanism that provides single axial displacement of the image sensor parallel to the principal optical axis, allowing for depth of focus adjustments and compensation. This design is fabricated and subjected to random vibration and thermal vacuum testing.

Table of Contents

List of Figures

List of Tables

I. Introduction

A. Setup

1. Background Information

Space exploration and space-based intelligence platforms often require complex optical systems to achieve their purpose. The idea of space-based optical systems was proposed as early as the mid 1940's by astronomer Lyman Spitzer (NASA, Telescope History, 2003). Decades later, NASA's Hubble Space Telescope became the first permanent space-based optical system to orbit the earth. It came at a cost of over $1.5 billion and required the use of the Space Shuttle Discovery to put it into orbit (Wertz, Everett, & Puschell, 2011). Figure 1A shows the approximate size comparison of the Hubble telescope to an average human being, for reference. That single mission has given scientists the most complete understanding of the universe to date and has been crucial in validating some of physics' greatest theories (NASA, Hubble Space Telescope, 2021). Future missions that include complex and expensive thermal solutions are still in the works. Most notably is the James Webb Space Telescope (JWST) which is scheduled to launch in late 2021. This telescope must remain at temperatures under 50 K (or -220 C) to protect its instruments (NASA, James Webb Space Telescope, n.d.). This is accomplished by employing a large sunshield, which measures approximately 14 meters by 21 meters (comparable to the size of a tennis court). The JWST is shown in Figure 1B.

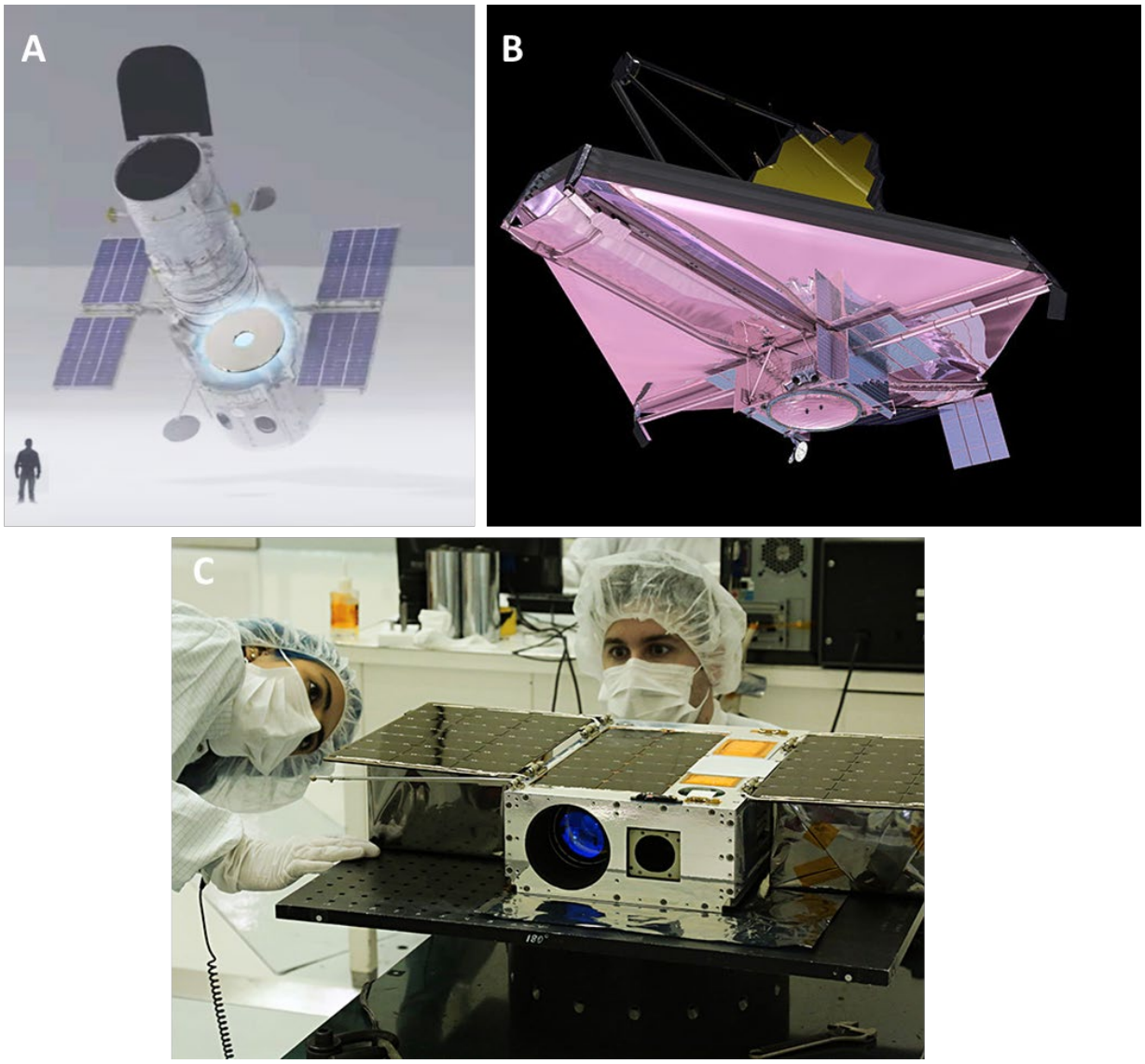

Figure 1: A) Size comparison between an average human being and the Space Hubble Telescope. B) The James Webb Space Telescope showing the underpinnings of tennis-court sized expandable solar shield. C) The ASTERIA (Arcsecond Space Telescope Enabling Research in Astrophysics) satellite.

Over time, space-based optical systems have continued to evolve, getting smaller and more complex. Today, many of these optical systems are launched by defense, security, and counter-intelligence agencies all over the world to keep their citizens safe. Additionally, a growing number of commercial entities have entered the market. One of the current trends in the space-based optical platform industry is to reduce the overall

size and weight of these systems to lower launch costs (Larson W. , 2006). At the same time, these miniaturized platforms are tasked with providing the community the same level of performance as legacy platforms, which are generally much larger and expensive.

One example of this is the ASTERIA (Arcsecond Space Telescope Enabling Research in Astrophysics) spacecraft, launched in 2017 as a joint effort between JPL and MIT. This spacecraft was JPL's first CubeSat that operated in space, with a mission duration of over two years. It weighs 12 kg and had lateral dimensions in the 20-30 cm range. Even at this size, ASTERIA provided valuable data and imagery to scientists in earth for the duration of its mission. ASTERIA was one of the first missions in its class to perform big science in a small package. The spacecraft is shown on of Figure 1C, above, while it was being developed in the JPL cleanroom.

One of the drawbacks of this trend is that making these platforms smaller brings forth new challenges in managing the ever-changing thermal environment in space. Generally, these platforms are exposed to direct radiation from the Sun, as well as thermal radiation from the earth for prolonged periods of time. This exposure to heat inputs can result in the need to manage temperatures as high as 150 °C (Wilson, 1999).

In contrast, when these platforms are behind the shadow of the earth, the thermal load is significantly reduced, and the payload temperature can drop to as low as -170 °C. To manage these fluctuating temperature challenges, current systems use large, expensive, and highly delicate thermal management systems. These systems consist of power-

consuming electronics, radiators, heat pipes and a combination of clever materials and surface coatings. Engineering such complex solutions into compact payloads creates a new class of performance challenges that must be addressed in high performance, space-based optical platforms.

A brief note on satellite sizes: NASA defines satellites based on their mass (Wertz, Everett, & Puschell, 2011). Large satellites have a mass greater than 1000 kg. Medium satellites have a mass between 500-1000 kg. Small satellites have a mass less than 500 kg. At times, it is helpful to further subdivide small satellites: mini (100-500 kg), micro (10-100 kg), nano (1-10 kg), and pico (less than 1 kg). The research presented in this thesis considers small satellites. At times, “nano” may be used to describe a particular small system.

2. Problem Statement

The commercial, defense, and intelligence communities have a need for space-based precision optical systems that deliver high performance across a diverse mission set and various thermal environments. The opportunity to address this need has become more apparent with the rapid acceleration of small satellite development. These small vehicles offer big opportunities in a compact space and at low prices. However, they cannot employ the traditional performance management systems of larger satellites, due to cost and SWAP (size, weight, and power) constraints. There is an opportunity to develop robust low cost and low SWAP mitigation strategies to enable optical systems with high

performance across a wide range of thermal and mission scenarios. A detailed analysis of the problem is examined in Section I.C.

3. Proposed Solution

The proposed low-SWAP solution is a single axis focal plane array focus mechanism. The mechanism is composed of a linear actuator that is attached to a flexure which holds the camera sensor while imaging. The mechanism allows for large changes in the focal plane while also maintaining the ability to make small adjustments for the best imaging data. This solution does the job at accounting for thermal gradients within the optical components that tend to degrade the image quality in a nanosatellite form factor, as well as providing the capability to adjust focus best based on distance to target.

4. Emphasis on Systems Approach

Moore's Law, which states that the number of transistors in an integrated circuit of a fixed volume roughly doubles every two years, has held true for half a century (Schaller, 1997). Fifty years ago, there were less than 100 transistors per square millimeter on an integrated circuit. Today, there are over 100,000,000 (Williams R. S., 2017). The growth of computational capability, along with its miniaturization, has fostered a similar boom in system complexity. This increase in complexity has had a comparable impact on nanosatellites, which now require similar systems engineering principles as their large satellite counterparts, but in a smaller form factor.

It is the intent of this thesis to address an engineering challenge through a systems-oriented approach. Emphasis will be placed not just on design and implementation

complexity, but on the requirements, expectations, and operation of the proposed solution.

5. Formation of the Thesis

The remainder of Section I covers contributors, a detailed analysis of the problem, and defines the success criteria of the proposed solution. Section II is an examination of the problem using a Systems Engineering approach. Section II defines key stakeholders, design constraints, operational scenarios, comparison of solutions, and develops a draft system requirement for the proposed solution, according to the Systems Engineering guides outlined in “Applied Space Systems Engineering” (Larson, Kirkpatrick, Thomas, Sellers, & Verma, 2018). Section III examines the Design Approach, both for the proposed solution and the required environmental testing that the unit will undergo as part of its qualification for relevant space requirements. Section IV consists of the environmental testing results and a discussion of the analysis. Section V provides recommendations for future work, throughout the design process (pre-test, during test, and post-test). Finally, Section VI concludes the work.

B. Contributors

1. Author Involvement

Jordan Karburn began working at LLNL in 2018 after graduating from California Polytechnic State University, San Luis Obispo with his Bachelor of Science in Electrical Engineering. Since 2019, Jordan has supported the LLNL Space Science and Security Program (SSSP) as both a technical design lead and project manager. His focus area is in electro-optical imaging systems. In addition to his other duties, he has been the lead

electrical engineering for developing a single axis focus mechanism for SSSP payloads. During his time at LLNL, he began pursuing his Master of Science in Electrical and Computer Engineering at the University of California, Davis. He is the project lead and primary electrical engineer for the work presented in this thesis.

2. LLNL/SSSP

"LLNL was founded in 1952 in service to the Department of Energy/National Nuclear Security Administration and other federal agencies. Leveraging the core competencies of x-ray physics, high-speed computing, advanced manufacturing, and advanced sensing technologies, LLNL's SSSP has used these competencies for advanced modeling & simulation, and the development of novel instruments.

LLNL has provided space payloads, including the gamma ray spectrometer–MESSENGER; x-ray optics–Solar Dynamics Observatory and NuSTAR; and imaging payloads–Clementine.

More recently LLNL has designed & constructed 18 space qualified imaging instruments since 2015 and has been executing three telescope Research & Development programs. LLNL has also been the lead for the GEOstare program which is an ongoing Nano-satellite prototype development collaboration between LLNL, Tyvak Nano-satellite systems to demonstrate mission utility from nano-satellite platforms for Space Situational Awareness. The project has flown its first prototype satellite, GEOstare SV1, with a second scheduled for launch Nov 2019.

LLNL developed the initial mission concept and was responsible for the design and development of the imaging payload." (Quintana, 2019)

3. Key Acknowledgements

In this master's thesis for Jordan Karburn, he was not the only one to contribute on the presented work. Cynthia Panas is a chief mechanical engineer at LLNL and is responsible for the mechanical design of the focus mechanism. John Cortes Gutierrez is a mechanical finite element analyst at LLNL, and he contributed significantly to the systems engineering effort. This project would not have been possible without their support and assistance.

C. Problem

1. Need for Precision Optics in Small Satellites

As the previous sections outlined, the potential uses of orbital telescopes are almost as varied and complex as their terrestrial counterparts. This research focuses specifically on optical imaging satellites. Such satellites are widely known, from famously expensive endeavors, such as the Hubble Telescope that has amazed the world for decades with images of deep space, to the mundane constellation of satellites, operated by Planet Inc, that enable Google Earth (Planet, 2021) and similar applications widely disseminating geospatial information.

Optical satellites faced the same challenges as every other sort of satellite: they are historically big, expensive, vulnerable, and have an exceptionally long development cycle (Larson W. , 2006). Thus, it is only natural that the proliferation of small satellites also impacts the optics industry. There is a place for multi-billion-dollar missions, such as the

Hubble Telescope, but there is also a place for a nanosatellite that can be deployed cheaply and quickly to address an immediate short-term need. An optical small satellite could be launched into a very particular orbit during a natural disaster, such as a wildfire, to provide rapid and expansive coverage that may not be available to the fleet of aircraft that would be required to cover the same range (Kaufman & Justice, 1998)

Given the constant improvements and miniaturization of image sensors and computing capability, the limiting factor for such a satellite to be economical is not the electronics, it's the optics. Thus, the need becomes apparent for precision optics, capable of delivering high performance images in a compact form factor.

2. Difficulty in Maintaining Performance

Assume for a moment that there are optics which exist that can provide the required performance in the necessary form factor. The difficulty then becomes maintaining that optics performance throughout a mission's life cycle. Changes in room temperature and vibrations in the air have noticeable difference on terrestrial optics performance (Bely, 2003)

The largest challenges for maintaining optical performance on orbit is twofold: thermal management and surviving launch conditions (Wertz, Everett, & Puschell, 2011). It is useful to further delineate the task of thermal management into two additional categories: challenges associated with coefficient of thermal expansion (CTE) and temperature gradients introduced into the optic via thermal exchange with its environment.

Both thermal management and launch loads are well studied and solved problems for conventional satellites. Solving these challenges in a cost-effective manner, while maintain low size, weight, and power (SWAP) is a new concept. Addressing these challenges is the focus of this thesis. Focus mechanisms can address the performance degradation associated with both launch and thermal environments.

3. Environmental Conditions

Spaceflight poses three distinct environmental challenges for any system operating in the vacuum of space: launch conditions, thermal management, and radiation. The purpose of this section is to provide a brief overview of each of these environmental considerations. Specific design constraints will be covered in Section II.C.

Launch conditions are the first hurdle any system must overcome. Generally, these can be thought of as two separate, but intertwined, design challenges: vibration and acceleration. For an object to escape the gravitational pull of another mass, the escape velocity (v_e) must be exceed. Governed by the equation $v_e = \sqrt{\frac{2GM}{r}}$, where G is the universal gravitational constant ($G \cong 6.67E^{-11}m^3kg^{-1}s^{-2}$), *M* is the mass of the body to be escaped from, and *r* is the distance from the center of mass of the body. The escape velocity of earth is roughly 11km/s, or 25,000mph (Wertz, Everett, & Puschell, 2011). Accelerating any object to such an enormous speed necessitates a rocky ride. The forces exerted on a system attempting to exceed the escape velocity are enormous, with acceleration values routinely several times that of earths normal gravitation pull of

~$9.82 m/s^2$. The SuperDraco rocket engines, designed by SpaceX, routinely reach accelerations of close to $30 m/s^2$ (James, Salton, & Downing, 2014). Mechanical structures undergo a huge amount of stress under such force. On a component level, it is not uncommon for solder joints to fail on electronics and for mechanical fasteners to sheer. In addition to the acceleration shock of a space vehicle, there tends to be considerable induced vibrations brought on by rocket propulsion. These large vibrations persist for several minutes and have been known to shake a vehicle quite literally to pieces (Hastings & Garrett, 1996).

The thermal environment of space is challenging. NASA provides the General Environmental Verification Standard as a baseline for environmental testing (GSFC-STD-7000, 2019)The vacuum (10^{-6} torr) will be sufficient to prevent convective heat exchange, leaving conduction and radiation. Convection is a primary method of cooling for terrestrial applications (i.e., air cooling on a laptop). Thermal management and dissipation is a vital and robust area of aerospace engineering. In addition to heat dissipation, there can be extreme temperature swings in an orbit Transitioning from illumination to shadow can cause very large thermal stress in a system (Gilmore, 2002).

Thermal effects present two challenges in optical systems: thermal expansion and temperature gradients. Thermal expansion occurs when structures expand and contract based on their temperature. The coefficient of thermal expansion (CTE) for each material is different. Therefore, assemblies with multiple materials will expand at different rates. This is particularly problematic in optical systems, where this mismatched expansion can

cause the system to go out of focus. Additionally, even in CTE matched systems, if the bulk structure is not subjected to uniform temperature change, there will be shifts that cause optical performance degradation (Burgh & Nordsieck, 2003). Sensors and electronics in the space vehicle (focal plane arrays, processors, communication units, etc.) distribute heat unevenly throughout the system. Temperature gradients can cause microscopic changes in the optic itself. For refractive elements (i.e., lenses), the index of refraction is correlated with the temperature of the material. If the material is not isothermal, the index of refraction will not be uniform throughout the optic, causing a divergence from intended optical prescription. Similarly, in reflective elements (i.e., mirrors), temperature gradients in the optic can cause non-uniform surface deformation. This deformation causes a similar deviation from the designed prescription of the optic, thus degrading overall system performance (Park, Chang, & Lim, 2020).

Last, but certainly not least, is the radiation exposure associated with space flight. Earth's atmosphere (and the magnetosphere) are very effective broad-spectrum radiation shields. The further away a space vehicle is from the shield, the greater doses of radiation one must contend with. Solar radiation has effects on practically all elements of a spacecraft, from damaging electronics to degrading material. While extremely important to consider, radiation management can be exceptionally expensive. Radiation management is largely driven by the required mission life and total budget. Because the primary goal of this research is to provide a low cost/low SWAP solution for small, inexpensive satellites, radiation consideration is generally omitted from this work (Wertz, Everett, & Puschell, 2011).

The proposed single axis focus mechanism addresses the problems of dynamic thermal conditions and mission varieties for small satellites. The focus mechanism can correct for focus shift during launch, compensate for thermal gradients, and set the optimal focus based on distance to target.

D. Purpose

LLNL has addressed the need of maintaining optical performance on orbit for nanosatellites by designing a single axis focus mechanism. This design was fabricated and underwent a first round of environmental testing.

E. Success Criteria

When designing any system, it is important to clearly define success criteria. The focus mechanism presented in this thesis was not designed as a purely research project. It is for a telescope being developed at LLNL. The tightly controlled mechanical, electrical, and optical system specifications and requirements are covered in depth in Section II.

The success criteria for the first-generation engineering unit (EU) presented in this thesis is a coarse pass/fail environmental testing event. During this test, the vibration performance of the system was evaluated. After vibration, the EU underwent thermal vacuum testing to determine its orbital survivability. If the unit was not explicitly damaged during these tests, it was considered a success. As this was the first-generation EU, no special attention was paid to pre/post characterization. Specific performance metrics were not of importance, such as power consumption or command execution. An exhaustive

comparison of pre- and post-test characterization was not performed or required. The EU did not need to meet every system requirement defined for the focus mechanism. Rather, this was a proof-of-concept for the approach taken in the design. Pre-test calibration and characterization was performed (and is presented), but only as an exercise in analysis.

II. Systems Engineering

The following section provides an examination of the systems engineering approach to addressing the needs of maintaining optical performance in small satellites, as described in (Larson, Kirkpatrick, Thomas, Sellers, & Verma, 2018). The section consists of an examination of stakeholder expectations, operational context and architecture, key constraints that drive the design, operational scenarios which must be considered during design, a comparison of potential solutions, a proposed solutions system architecture, and a draft of the system requirements for the solution.

A. Stakeholders and Expectations

A summary of the stakeholders, as well as their active / passive designation is listed in Table 1 below. These stakeholders represent anyone or anything that interacts with our space-based optical system or has an interest in its success. We explore each individual stakeholder and their expectations below.

Stakeholder	Role Type
LLNL Project engineers (design, mechanical, electrical, optical)	Active
Project sponsor	Sponsor / Passive
Scientific and/or defense end user	Active
Launch partner (s)	Active

LLNL management	Passive
Optical system component (lenses, monolithic telescope, cameras, sensors, power supply, etc.)	Active
General public / taxpayers	Sponsor / Passive

Table 1: Stakeholders and their roles for the Low SWAP space-based optical system solution.

1. LLNL Project Engineers (Critical Stakeholder)

This is the Lawrence Livermore National Laboratory team that will be in charge of delivering the final solution to the end user, which could be a defense agency, scientific user, or another team within the Laboratory. This team includes engineers from all fields, including mechanical, electrical, materials, among others. This stakeholder is considered critical because they are responsible for delivering a system that will meet the expectations of the end user, LLNL management, sponsors, and the general public. Their expertise is heavily relied upon to design, validate and build the best possible solution with a given set of resources. This team will also be relied upon by the end user to provide support and technical guidance during the duration of the mission.

Expectations:

- Mission parameters should be clear. This includes information such as orbit parameters, launch conditions as well as other factors that may influence the thermal and optical performance of the final system.
- Cost constraints should be clearly communicated to the LLNL project engineers. This will allow them to make decisions on how to best use time and resources to accomplish the goals and meet the mission requirements.

- A project timeline should be provided so that the LLNL project engineers can account for man-hour allocation and prioritization among other competing time-sensitive projects going on at LLNL.
- The requesting team of sponsors (defense or scientific) will keep the LLNL team up to date with any changes in regard to mission parameters, expected cost or timeline modifications.

2. Project Sponsors

This is the team that is in charge of providing the majority of the funds for the project. The sponsor for these types of space-based optical systems often includes (though not limited to) the National Aeronautics and Space Administration (NASA) and other United States Federal agencies.

Expectations:

- The system will deliver a high-level optical performance under the prescribed mission parameters, which include thermal fluctuations, vibration during launch and expected mission duration.
- The system will provide comparable performance to larger, more expensive platforms while maintaining a low size, weight, and power (Low-SWAP) approach.
- The system will be fully designed and developed within the budget constraints provided by the sponsor.
- The system will be delivered by the date required by the sponsor with all efforts made to avoid delays. If there are delays, the LLNL team should communicate with the sponsor to find the most realistic timeline.

3. Scientific and Defense End Users (Critical Stakeholder)

This is the team that will ultimately be the end user of the data collected by the system. This group of stakeholders may include scientists doing atmospheric or astrophysics research as well as defense teams tasked with keeping the nation and its interests safe from adversaries. This is a critical stakeholder because they require the best possible data from the system (such as photos) to make crucial national security decisions and novel discoveries.

This stakeholder is also in charge of sending instructions to the system regarding where and when to take photographs for the duration of the mission. This is the stakeholder that will likely interact with the system the most after it has been launched.

Expectations:

- The end user needs the optical data to be reliable and of high quality, comparable to that which they have received from much larger and expensive space-based optical platforms in the past.
- The final image must be in focus so that it is easy to characterize and draw scientific or informative conclusions form it.
- The end user expects that the cost of receiving the data will not be any higher than the cost of data from previous legacy platforms.
- The data received from the platform should not be in any way distorted or affected by thermal issues aboard the payload while in space.

4. Launch Partner

The launch partner is tasked with preparing the payload for launch aboard their own platform. They make sure that the final design meets are launch specifications, including weight and final form factor. The launch partner delivers the optical space-based optical system to its final position in orbit aboard a rocket.

Expectations:

- The final system meets all launch criteria. In particular it must meet the maximum weight allowed by the launch vehicle's capabilities.
- The final system must not be larger than the required dimensions and must be designed to fit within the given payload attachment points.
- The final system will be designed with a safety-first approach that will not put any of the other payloads or launch rocket at risk during launch and deployment. It will also be designed with the safety of humans who interact with it in mind.
- The final system will be safe for the launch partner's engineers and technicians to work on while testing and preparing the platform for launch.

5. LLNL Management

This stakeholder includes all Lawrence Livermore National Laboratory (LLNL) management team members involved in ensuring the final system is safe and meets the high scientific standard of the Laboratory. LLNL management imposes constraints upon the design team to make sure safety and national security are prioritized during the development process.

Expectations:

- The Lab health and safety standards will be met during design, test and deployment of the space-based optical solution.
- The final design will continue the lab's excellent history of delivering functional and high-performance scientific instruments to the United States (or approved ally) sponsor community.
- The final design will have no negative impact upon the Lab's mission of maintaining national security as a top priority.
- Safety notes will be written and documented in the LLNL ELM system as necessary to ensure that the systems are safe to use and test within Lab sites.

6. Optical System Components (Critical Stakeholder)

This stakeholder represents the components that will make up the system. They include lenses, cameras, electronics, sensors, focus mechanisms, power supplies, power converters, heating elements, thermocouples, processors, communication devices, mirrors, and other key components. They interact with each other, as designed by the engineering team, to capture and relay optical data to the end user.

This is a critical stakeholder because it is tasked with taking the actual images that will be delivered to the end user and other interested stakeholders. The mission depends solely on the continued function of these components.

Expectations:

- The optical components require careful consideration in regard to thermal management. They should be kept within a set temperature range to perform at

their best. Generally, lenses, mirrors and monolithic telescopes can experience deflections and changes in index of refraction due to thermal gradients, degrading their optical performance.

- The optical system components will be shielded from the harsh vibrations experienced during the launch procedure. They will also be engineered to withstand the high g-force loading experienced at launch.
- The system will be properly shielded to protect it from minor collisions with small pieces of space debris while on orbit. This will ensure that the optical system can deliver quality data for the expected duration of the mission.

7. General Public

This stakeholder is a taxpayer whose taxes will be used to fund much, if not all, of the project. They may have an interest in scientific advancement as well as keeping their country and families safe through defense programs looking to use our space-based optical systems.

Expectations:

- Their taxpayer money will be used wisely to fund projects that will result in them being safer and / or making novel discoveries that advance the base of scientific knowledge.
- They expect the sponsor to hold the LLNL engineering team accountable for all aspects of the design of the final system.
- The final system should be safe to operate in orbit and not put the health and safety of the general public at stake during and after the mission.

B. Operational Context and Architecture

1. Context Diagram

The interaction between the various stakeholders is described in detail in the context diagram presented in Figure 2. The optical system depends on key inputs from several active stakeholders, including the end users, LLNL engineers, launch partners and the optical components that play a key role in the system. The LLNL engineering team designs and develops the Low-SWAP spaced based optical system using in-house expertise and the facilities available here at the Lab. When it is fully ready, the LLNL team delivers the launch payload to its launch partner, which is tasked with testing and validating that the system will be able to withstand the launch and the environment while it is in orbit accomplishing its mission.

The launch partner will test the payload for thermal management performance through thermal cycling and provide the data back to the LLNL design team. The LLNL design team, in return, provides guidance and system expertise to the launch partner during the preparation phase.

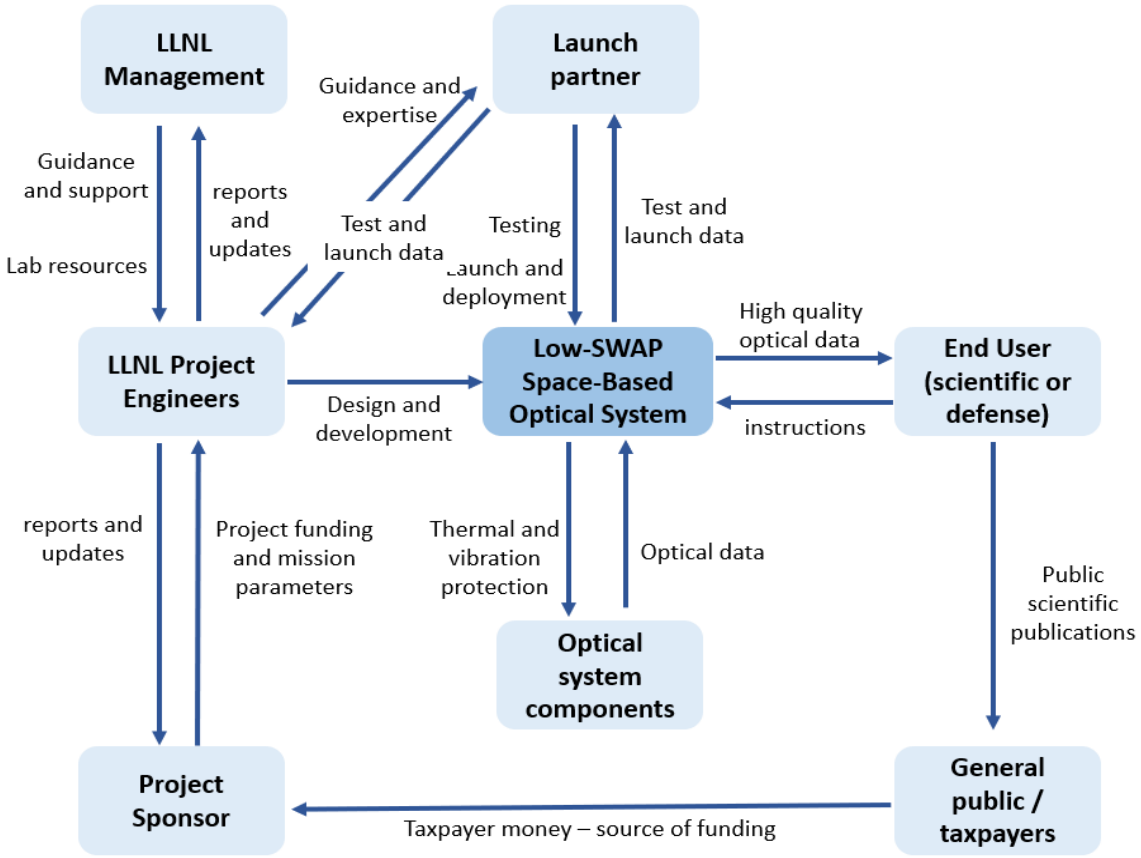

Figure 2: Context diagram showing the detailed interactions between the system and the various stakeholders.

The LLNL engineers are in continuous communication with both the sponsor community and the Lawrence Livermore National Laboratory management team. Generally, both of these passive stakeholders will require either monthly or quarterly reports, though this may vary by team or sponsoring agency. In return, the sponsor adds continuous sources of funding to the project (often on a yearly or contractual basis).

The individual optical components relay the optical data into the overall system to be transmitted to the end user. In return, the system provides these often-fragile components with protection from the Sun's radiation, high-fluctuations in orbit temperature as well as vibration protection during launch.

C. Constraints

1. Environmental Survival and Operational Conditions

Space systems are generally subjected to extreme environmental conditions, for both survival and operational expectations. These conditions greatly restrict the potential options, both at the component and subsystem level, that are suitable to a part of the solution.

2. Focal Plane Array (FPA) Compatibility

Basic solutions should be versatile and not require significant redesigns for every FPA implementation, especially those in the same "family", i.e., visible imagers with a common spectrum sensitivity. This is largely derived from the cost constraints inherent with small spacecraft. Solutions which are not scalable tend to be infeasible.

3. Mission Orbit

The mission orbit dictates several factors that limit the solution space. The orbit determines the frequency and duration of eclipse, which in turn significantly impacts both the power available to the space vehicle and the environmental conditions that it must survive. The mission orbit is the single largest thermal driver for a given payload.

4. Volume

By their very nature, small satellites have very limited volume. CubeSat formfactors are limited by standard dimensions (i.e., 1U, 3U, 6U, etc.). This is not just the norm, or

convention. Rather, many launch vehicles have non-negotiable fixed volume standards that the space vehicle must adhere to. Therefore, any system is inexorably constrained by the available payload volume.

5. Mass of Solution

Mission price tag closely relates to mass. In fact, it is not uncommon for the cost of a mission to be conveyed as price per kg. In addition to the cost associated with additional mass, there are survivability constraints associated with mass. Generally, space missions are subjected to extreme structural loads during launch. The center of gravy (and center of mass) of a payload are important. Imbalanced payloads represent a potential hazard to the space vehicle.

6. Mass of FPA

The mass of the FPA in the system obviously impacts the overall mass of the system. However, in addition to the general mass constraints discussed previously, the mass of the FPA impacts the structure required to hold the FPA during launch. Heavier FPAs require greater forces to resist deformation during launch, representing significant mechanical design challenges.

7. Power

Power on small satellites is very limited. All solutions must adhere to a strict power budget. Those solutions which require large amounts of power, such as active thermal management, represent risks to potential orbits that can be supported.

8. Schedule (long lead)

Small satellites should be agile/low lead time. The solution cannot be a significant driver in overall payload development/deployment schedule. Custom fabrication or exotic components constrain the missions that this solution support with short notice.

9. Material Selection (outgassing)

All materials must be safe for vacuum. Corrosion resistant, low outgassing, failure of material should not impact other subsystems. A common method of constraining this choice is the total volume and total mass loss of a system after extended exposure to vacuum.

10. Electrical Design Selection (radiation hardened)

Depending on orbit/mission life/risk tolerances, radiation hard or tolerant electrical components may be required. Not only does this greatly impact cost and schedule, but it also significantly impacts the potential electronics that can support a solution. Most integrated circuits are not available in rad-hard alternatives. Thus, designers are limited to a select pool of components that have been adequately qualified.

11. Coefficient of Thermal Expansion (CTE)

Precision optical systems are very sensitive to alignment. CTE mismatch in material causes system to go out of focus in difficult-to-correct manners.

12. Cost

Small satellites are generally heavily constrained by cost. If cost weren't a factor, then the satellite would not be required to be small. Solution must fit in general low-cost small satellite design paradigm.

13. Launch Conditions

Launch conditions dictate shock and vibe requirements. Launch vehicles vary significantly when it comes to expected environmental conditions during launch. Regardless of the specifics, these conditions are likely to be extreme. The two biggest drivers are the impulse shock of engine ignition, as well as overall vibration during early boosting stages. These loads can be enormous, tens or hundreds of times earths normal gravity. Any precision optical system must withstand launch conditions while maintaining optimal focus. Due to risk mitigation, it is unwise to rely on system to re-focus after launch, pending any other system failures.

14. Bus support

In order to create a versatile solution that is compatible with a variety of missions, space-vehicle support and compatibility must be taken into account. The portion of the space vehicle that supports the science payload is known as the bus. Several bus inter-dependencies exist, from the manner in which the payload is mechanically integrated to the structure to the expectation for electrical interface. These parameters vary significantly from bus providers. Any solution must be as design agnostic to avoid bus-dependencies.

15. Timing

The speed at which the system can be refocused largely impacts the sort of solutions applicable. For systems that wish to autofocus based on the distance to target, rapid response times may be required. This constraint limits the sort of mechanisms capable of focus compensation. For especially rapid requirements, an autofocus schema may be required.

16. Minimum Required Displacement

The optic in front of the FPA generally sets the minimum required displacement to bring the system back into focus. Back focal length is determined by the focal length and aperture of the system, as well as a few other parameters of the optical design. The back focal length is generally well below 100um and sometimes as small as single digit micron. For precise control, the corrective system must be able to compensate to small percentage of an optics back focal length.

17. Displacement Certainty

Regardless of the minimum required displacement, there must be some confidence known regarding the position of the FPA. Generally, the minimum value of this constraint is on the same order of precision as back focal distance. This will provide feedback to the users of the system whether or not the optic is in focus.

18. Manufacturability

Any focus system should support the principal payload and should not represent a significant design risk. Many exotic designs exist, employing novel material properties or mechanical design, that are simply too difficult or too expensive to manufacture in an affordable manner. Therefore, any solution for focusing low SWAP precision optical systems must themselves be relatively simple and easy to manufacture.

19. Repeatability of Control

Any system must be highly characterized and repeatable in order to provide confidence in its solution the various environments that will be required in orbit. The solution therefore is constrained by its repeatability across environments. Low system-hysteresis, uncertainty, and high repeatability dictate the potential solution space.

D. Quality Functional Deployment (QFD) Matrix

WHATs - Stakeholder Characteristics	HOWs - System Objectives	Number of custom components	Total number of components	Minimum displacement adjustment	Maximum displacement rate	Number of compatible FPA	Total range of displacement	Number of required vendors	Total volume lost of materials	CTE difference of materials	Percentage of solution mass	Average orbital power	Importance: 5 High, 1 Low
Low cost		+++	+	+	+	+	+	+	++		+	+	5
Low volume					+	++	+++						3
Low mass						+	+			+	+++		3
Low power												+++	2
Short lead time		++	+	+				+++	+++				3
Radiation hardened								+	+			+	1
Survive thorugh launch				+	++		+				+++		5
Versatile with various optics		+++	+	+	+	++	++	++		+			4
Easy to manufacture		++	++	+	+	+	+	+++	+	++			2
Feature Raw Score		96	18	19	29	31	54	63	45	13	77	24	

Table 2: Quality Function Deployment (QFD) matrix. Weighted and summed scores are presented at the bottom.

The Quality Functional Deployment matrix, shown above in Table 2, is a useful tool to translate desired system characteristics into nonfunctional system requirements (Larson, Kirkpatrick, Thomas, Sellers, & Verma, 2018). It's goal is to ensure system requirements address the stakeholder expectations in an appropriate manner. The "HOWS" of the system are weighted against the "WHATS" of the system. Stakeholder Characteristics are given an importance value of 1-5. The Feature Raw Score is a summation of the weighted impact of the "HOWS" with respect to the "WHATS". The highest important weight (+++) is valued at 9. The medium impotant weight (++) is valued at 3. The lowest importance (+) is valued at 1. The exact weighting and importance level are tuneable. By nature, the QFD is meant to be iterative and recursive.

E. Operational Scenarios:

1. Earth Observation (EO)

A common mission type for optical satellites is known as Earth Observation. In these missions, the payload is pointed towards the earth. The focus for these requirements is generally fixed at infinity. That is to say, the optical system is trying to resolve images that are at the far extreme of its focus range. The only adjustments generally required for Earth Observation missions are when the system goes out of focus due to thermal expansion or contraction of the satellite.

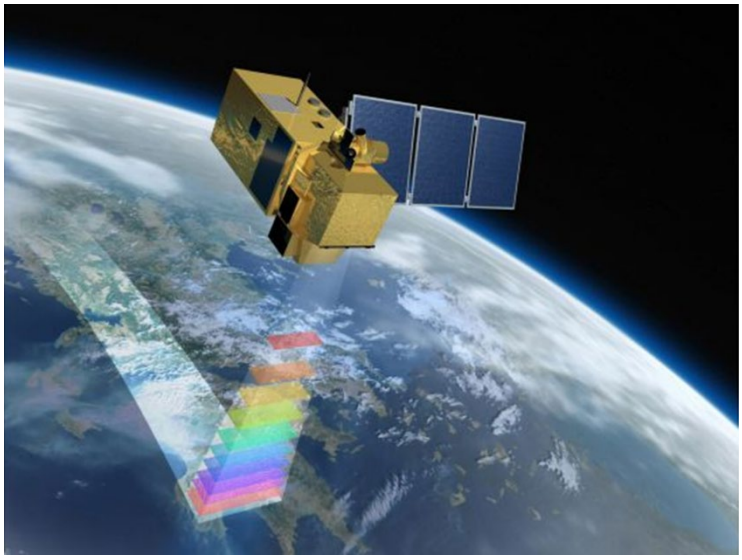

Figure 3: Graphic depicting a potential Earth Observation mission. (International, 2017)

Depending on the particular orbit of the satellite, there may be frequent and/or extended periods of time where the system is in eclipse: the earth is entirely blocking the sun from the field of view. This causes extreme temperature fluctuations in the system, often greater than 50°C (Wertz, Everett, & Puschell, 2011). While it is unlikely to be required to take images of the earth during eclipse, as there is very limited light available for the sensor, the structure itself still undergoes thermal expansion and contraction. This can cause the depth of focus to shift, and thus, for the system to go out of alignment.

2. Solar System Science

Very similar to EO, Solar System Science exclusively views objects at the maximum focus range. This is the sort of mission that observational telescopes perform, such as the NASA Hubble or Kepler telescopes.

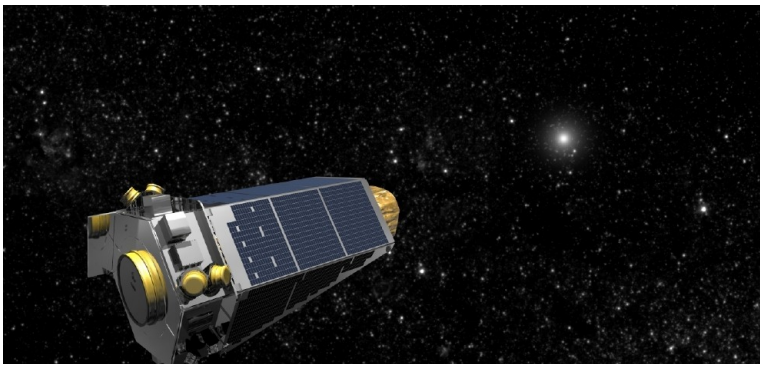

Figure 4: Kepler Telescope, an example of a Solar System Science Mission. (Dunn, 2016)

There is no reason for these systems to ever focus on objects closer than the maximum range. However, as with EO, eclipse can significantly impact the performance of a telescope on a Solar System Science mission. Unlike EO, an SSS mission may be taking images during eclipse, meaning the cold/hot cycling of the orbit can significantly alter the depth of focus, depending on the thermal isolation of the optical payload. Therefore, it is critically important to be able to control either the thermal environment or the depth of focus of the optic.

3. Space Situational Awareness (SSA)

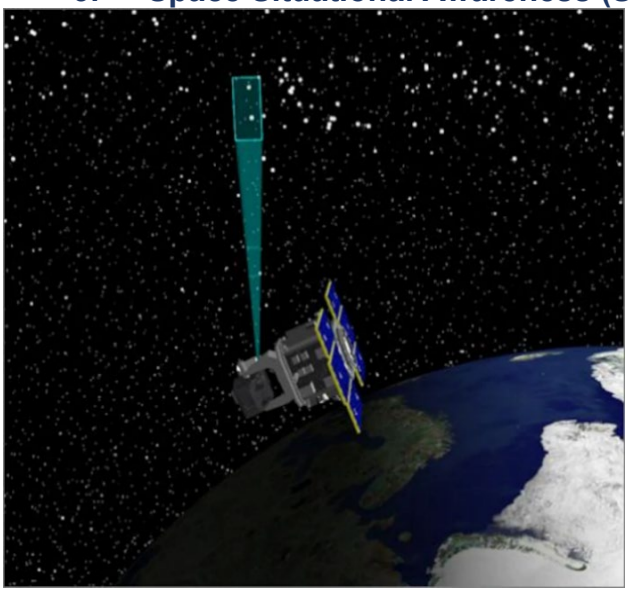

Figure 5: SSA satellite observing and characterizing space debris. (Williams K. , 2013)

SSA missions represent the most challenging operational scenario of the three presented. SSA payloads may be required to focus on objects at the maximum range of the system; they may also be required to focus on images significantly closer. All of the problems associated with thermal extremes introduced by orbit-dependent eclipses still apply. In addition, SSA payloads must have active focus, similar to a consumer digital camera, if they wish to resolve objects at a variety of distances. Due to the relative groundspeed of spacecrafts (approximately 7km/s), several focus adjustments may be required to happen in very short time frames. Not only must the system be able to compensate for overall focus on small scales, but it must also do so rapidly and across large ranges of travel. The required range of travel is a function of certain optical system parameters, such as the focal length and optical aperture.

F. Sequence Diagrams:

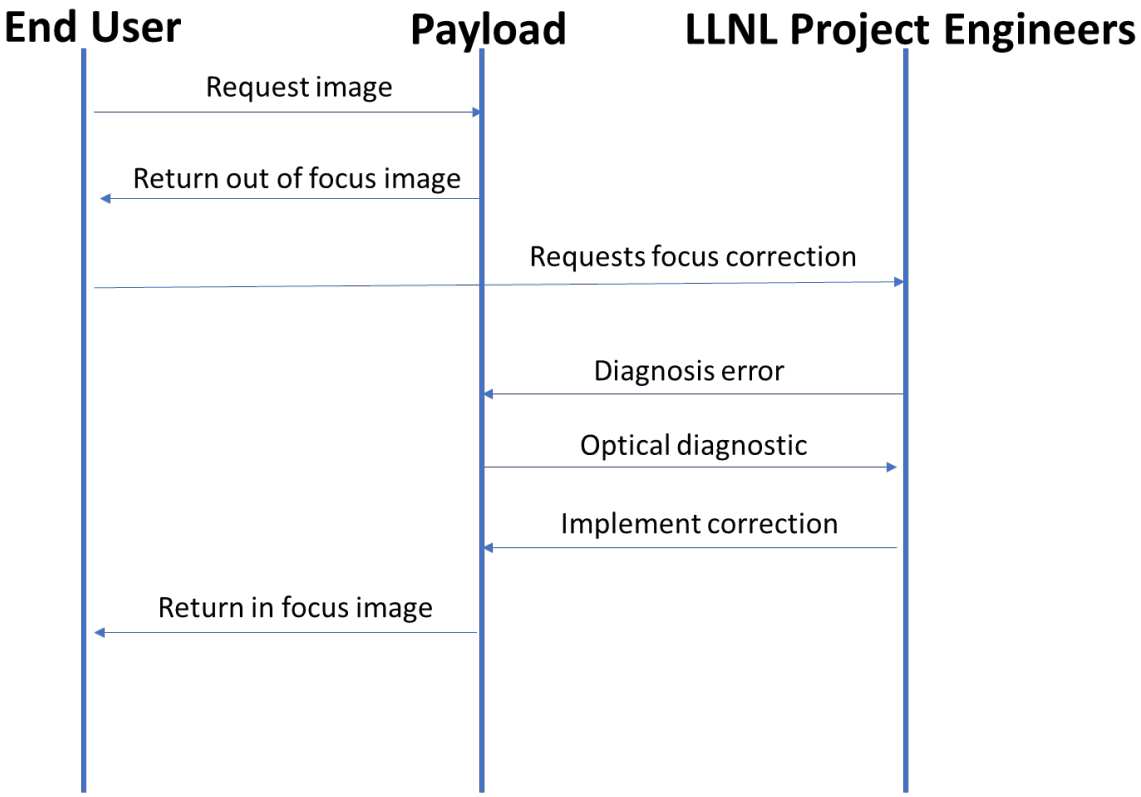

Figure 6: Sequence diagram depicting an Earth Observation mission process flow.

This sequence diagram describes the events of an Earth Observation or a Solar System Science mission. The End User requests an image from the Payload. Due to thermal shift, the Payload may return an out of focus image. The LLNL Project Engineers would then analyze the image and determine the source of the error. This may involve some back-and-forth diagnostics with the Payload. Once the issue has been identified and resolved, the Payload can return the requested image to the End User, now in-focus.

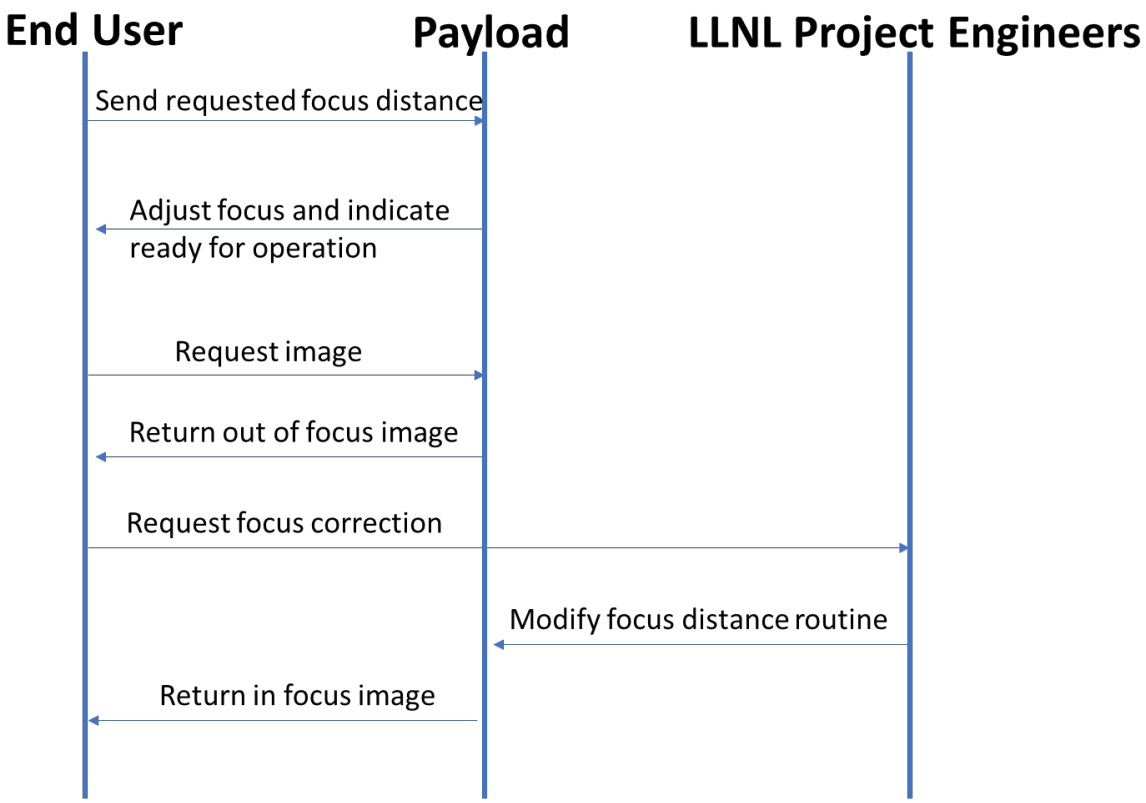

Figure 7: Sequence diagram depicting a Space Situational Awareness mission process flow.

This sequence diagram describes the events of a Space Situational Awareness mission. Instead of the Payload being at a fixed distance to target focus, constant focus adjustment is required. This would generally manifest itself as the End User sending a distance to target to the Payload. From there, the Payload would adjust its back focal distance until it believes itself to be in focus for the target of interest. When the End User requests an image at that distance, it is possible the Payload may be out of focus. This could be because of a miscalculation or uncertainty in distance to target, or because of thermal shift. The End User would contact the LLNL Project Engineers who would once again diagnosis and correct the issue. Finally, the Payload would be able to return in-focus images for a target at a provided distance.

G. Implementation Concepts Selection and Rational

1. Active thermal management

This solution involves the use of active heating and / or cooling elements surrounding the system. These components are strategically placed around the optical components to provide temperature control and minimize thermal gradients that degrade the quality of the optical data output. Figure 8 shows a simple diagram for this candidate solution. The control unit sends and electrical input to the heater / cooler in order to provide a thermal input to the system. A set of temperature sensors, which are attached to the optical components, provide feedback to the control unit, forming a closed loop system. This solution is complex and prone to failure due to the increased number of electrical components. It also requires additional space in and around the payload to work. Although it provides the best temperature control, it can be slow to react to large temperature changes (such as exposure to the Sun or shadow) and it can also be quite expensive to implement. The heating elements also require large amounts of power, which are in conflict with weight and size constraints placed upon the overall payload. This solution does not address the potential need for large changes in focus plane. It merely mitigates the potential distortions from thermal gradients within the optical components (Bely, 2003) (Bennion & Thornton, 2010) (Hastings & Garrett, 1996).

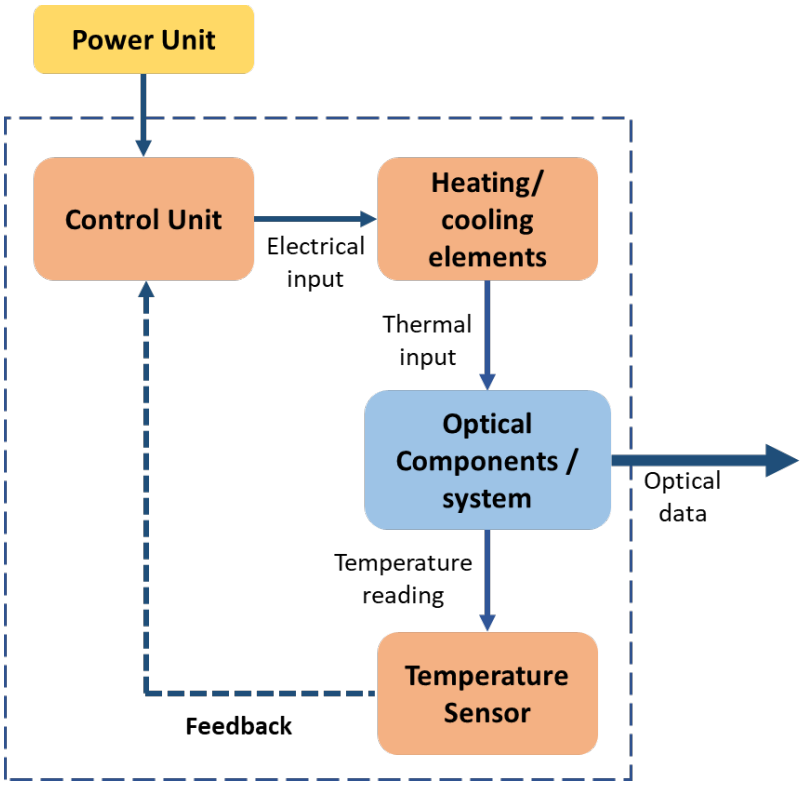

Figure 8: Diagram for the active temperature control solution. This solution is based on using a closed feedback system to maintain a consistent thermal environment for the optical components using heaters / coolers and temperature sensors.

2. Passive thermal management

Another way to minimize the thermal gradients within the optical components is to strategically select materials that insulate the components from external heat inputs. Additionally, reflective coatings and low-emissivity coatings can be used throughout to reduce radiative heat transfer to the optical components and associated electronics. The key benefit of this solution is that it reliable. The materials would be space-grade, so that they do not degrade in the harsh space environment. On the other hand, there are several drawbacks associated with this alternative. The solution is not able to adapt to potential changes in the spacecraft environment. It provides no control if unknown situations arise, leaving the possibility of low-quality data as a result.

Similar to alternative 1, this solution cannot account for large changes to the desired focal plane, especially if that change is particularly large. This solution would only work for very specific orbits and very specific targets to be imaged. It would limit the versatility of the system. Figure below shows a simple diagram of the optical system insulated and coated by smart materials and insulating coatings (Werner, 2012).

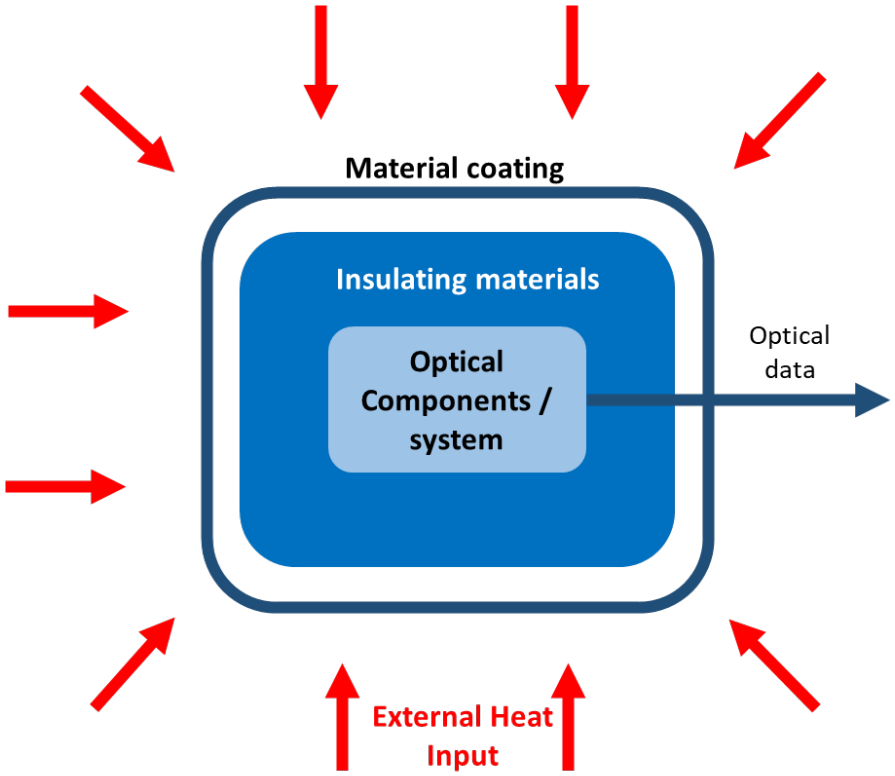

Figure 9: Diagram for the passive thermal management solution which is made up of smart material choice and thermal coatings to reduce thermal inputs into the optical components.

3. Deformable MEMS FPA

There exists the possible to create a microelectromechanical system (MEMS) that can deform the focal plane array (FPA). Ongoing work in high fidelity MEMS structures is an area of great interest in both academia and industry (Madec, 2012). With this approach, the position of the individual pixels would be controllable (Jahn, et al., 2016). Instead of a fixed FPA, acting as a monolith, elements of the array would be adjusted with either tip, tilt, or piston. Such control over the FPA would provide an enormously robust optical system, capable of compensating for a plethora of optical aberrations (including de-focus).

However, the technology readiness level (TRL) of such an approach is extremely low, especially in small satellites. As of this analysis, such an array does not exist at an experimental level, let alone as a readily procurable solution. Any system which would want to pursue such a technology would require a significant investment in both time and capital. Additionally, even if such a sensor was created, it would be intrinsically tied to a particular sensor. In many aspects, this approach is creating its own FPA. Fundamentally, this limits the versatility of such an approach (Dinyari, Rim, Huang, Catrysse, & Peumans, 2008).

4. Optical System Focus Control

Adjusting the spacing of the primary and secondary mirrors in Cassegrain reflective telescopes can compensate for radially symmetric focus shift parallel to the optical axis.

It is possible to have both active position control of the primary and or secondary mirrors. However, this method of focus compensation has significant drawbacks. First and foremost, a high performing optical system is extremely sensitive to alignment tolerances. Allowing for a degree of freedom to accommodate axial movement introduces the potential of tilt or tip of either mirror. Though there are mitigating strategies that could help avoid tip/tilt, they are difficult to implement. The spacing of the primary and secondary mirror is also required to be precise to hundreds of nanometers. Therefore, it is a difficult variable to control dynamically. Additionally, the design is heavily dependent on an individual optics mechanical design. Certain telescopes do not allow access to the primary/secondary mirror spacing. Those that do generally employee mission-unique mounting schemes. Therefore, it would be extremely difficult to find a design that could be versatile for a variety of missions (Burgh & Nordsieck, 2003). Figure 10 shows a diagram of this approach.

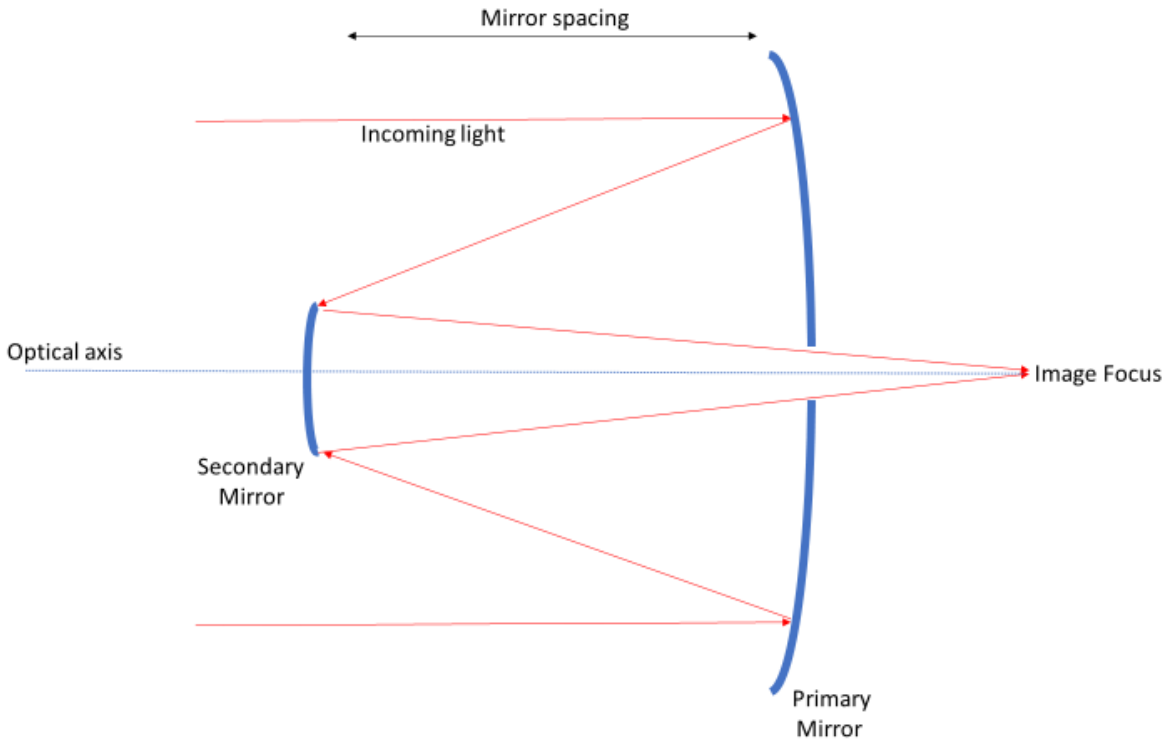

Figure 10: Diagram for the optical system focus control alternative. It is based on the idea of changing the distance between the primary and secondary mirror to adjust the focal plane of the camera.

5. FPA Focus Control

Another option for controlling radially symmetric focus shift is changing the position of the focal plane array at the image focus. Instead of adjusting the primary/secondary mirror position, it is possible to adjust the position of the sensor. This has significant benefits over modifying the mirror spacing directly. Importantly, the tolerances for adjusting the focal plane array position are significantly less stringent than the mirror spacing. Typical depth of focus tolerances are tens of microns, compared to hundreds of nanometers. There are several actuators that are capable of this precision that are also low power draw. An added benefit of lower required displacement specification is increased range of travel.

However, one major drawback of this method is that the FPA can be quite heavy, relatively speaking. A heavier FPA means that the mechanism must be capable of holding the mass of the FPA during launch loads, which are frequently tens of times greater than gravity. There are design challenges in attempting to combine high precision, small adjustment, and large axial-loading capability (Bely, 2003) (Fiete, 2010).

H. Pugh Matrix

	Alternative 1	Alternative 2	Alternative 3	Alternative 4	Alternative 5
Criteria	Active Thermal Control	Passive Thermal Control	Deformable MEMS FPA	Optical Focus	FPA Focus
Low Size	S	-	+	-	S
Low Weight	S	-	+	-	-
Low Power	-	+	S	-	S
Low Cost	-	-	-	-	+
General-purpose/reusable	-	-	+	-	+
Low complexity	S	+	-	-	+
Mechanically robust	+	+	-	-	S
Compensate for defocus	S	S	+	S	S
Compensate for distance to target	-	-	-	S	S
$\Sigma +$	1	3	4	0	3
$\Sigma -$	4	5	4	7	1
ΣS	1	3	4	7	4
Total	-3	-2	0	-7	2

Table 3: Pugh Matrix comparing the possible alternative solutions.

A Pugh Matrix, as shown in Table 3 above, is a qualitative tool meant to aide in the decision process for multi-dimensional systems *(Pugh, 1981)*. The criteria, shown on the far left, are derived from stakeholder expectations. Each Alternative Solution is detailed along the top of the Matrix. All alternatives are evaluated against the stakeholder criteria. There are three possible weights assigned in the matrix: “+”, “- “, and “S”. “+” implies the alternative exceeds expectation for a criterion and is given a value of 1. “–“ implies the alternative offers inferior performance for a criterion and is given a value of -1. “S” implies the alternative is satisfactory in a criterion and is given a value of 0.

.

I. Proposed System Operational Architecture:

Based on the Pugh Matrix provided in the previous section, the “FPA Focus” approach appeared to provide the best performance against the stakeholder criteria. Figure 11, below, proposes a three-level decomposed System Operational Architecture for the FPA Focus System.

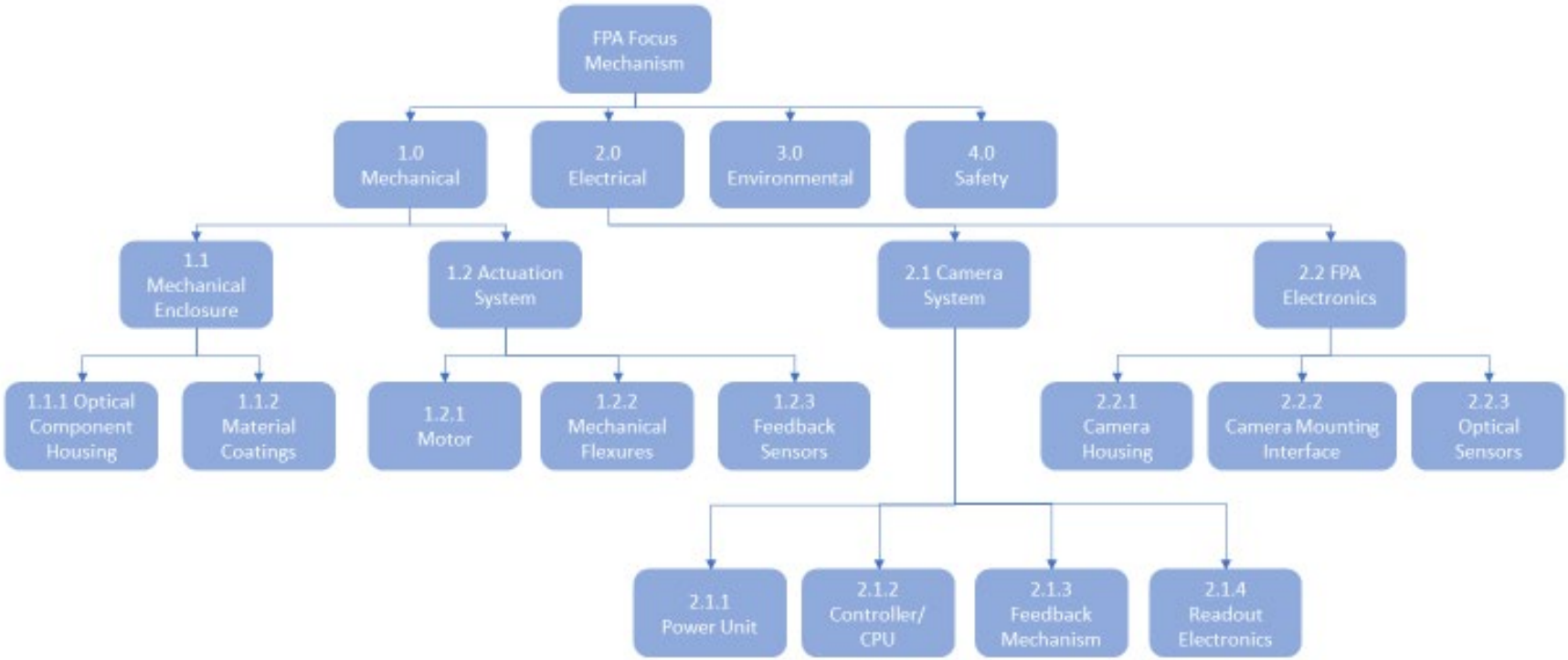

Figure 11: Diagram of the FPA Focus system architecture.

J. System Requirements:

The following provides derived System Requirements for the FPA Focus Mechanism. These are the requirements which the Focus Mechanism would adhere to for a fully compliant system. The four sections (Mechanical, Electrical, Environmental, and Safety) are structured based on the first level decomposition of system architecture. Subsequent numbering ID (i.e., M.1.0) are for ease of reference and do not correspond to second level architecture structure.

Note: the engineering unit (EU) presented in the following two sections is not expected to adhere to all requirements, as it is a development unit. The EU serves to inform future designs, allowing them to be compliant with all requirements.

1. Mechanical

ID	Description	Rationale	Verification Method
M.1.0	The focus mechanism shall withstand the mechanical stresses induced by the launch procedure and operation.	Required for operation and mission success.	Test and Demonstration
M.2.0	The focus mechanism shall withstand stressed derived from thermal gradients experienced during launch or operation.	Required for operation and mission success.	Test and Demonstration
M.3.0	The focus mechanism shall have a minimum step resolution of 10 μm with a goal of 5 μm (± 10% is acceptable).	Required for fine adjustments in the designed focus plane during imaging.	Test and Demonstration
M.4.0	The focus mechanism shall have a minimum range of linear travel of 4 mm, with a goal of 10 mm.	Required for changing the focus plane of objects at varying distances.	Test and Demonstration
M.5.0	The focus mechanism shall have a maximum rate of linear displacement of 2 mm/s.	Required for making timely changes to the focus plane.	Test and Demonstration
M.6.0	The focus mechanism shall contribute minimally to the thermal load of the payload.	Required for continued operation and mission success as well as health of electronics and other critical components.	Test and Demonstration
M.7.0	The focus mechanism shall withstand the vibration spectrum during launch procedure	Required for components to remain as assembled during operation.	Test and Demonstration
M.8.0	The focus mechanism shall hold 0.5 kg camera during launch procedure without failure.	Required for components to remain as assembled during operation	Test and Demonstration
M.9.0	The focus mechanism shall be compatible with the camera system	Required for system compatibility and proper assembly.	Test and Demonstration
M.10.0	The system shall have a first mode natural frequency of no less than 60 Hz	Required for operation and mission success.	Test and Demonstration
M.11.0	The system shall not have any response modes from 105-135 Hz with greater than 5% mass participation.	Required for operation and mission success.	Test and Demonstration

Table 4: Mechanical System Requirements

2. Electrical

ID	Description	Rationale	Verification Method
E.1.0	The focus mechanism shall consume less than 10W	Required to meet low power constraint of small satellite	Test and demonstration
E.1.1	The focus mechanism shall have an inrush current of less than 6A for 100ms	Upper bound of inrush current supplied by conventional batteries	Test and demonstration
E.1.2.0	The focus mechanism shall operate at one of the nominal voltages, provided by the bus, either 3.3V, 5V, 12V, or 28V	Standard voltage range provided by spacecraft bus	Test and demonstration
E.1.2.1	The focus mechanism shall operate at an under/overvoltage rating of at least $\pm 10\%$ and survive an under/overvoltage range of at least $\pm 20\%$	Voltage levels fluctuate, depending on orbit and battery life, and focus mechanism should be able to withstand those events	Test and demonstration
E.2.0	The focus mechanism shall accept commands over an RS-422 link at 1Mbps baud rate	Standard method of communication for bus interfacing at an appreciable rate	Demonstration
E.2.1.0	The focus mechanism shall provide telemetry feedback to the bus over an RS-422 link at 1Mbps baud rate	Standard method of communication for bus interfacing at an appreciable rate	Demonstration
E.2.1.1	The telemetry shall, at a minimum, include current position, any queued commands, and temperature of the actuator	Telemetry packets contain critical information for mission assurance	Demonstration
E.3.0	The focus mechanism shall provide the absolute position of the FPA, relative to the exit pupil of the optic, via feedback mechanism to a precision no less than 5um at a rate no less than 1Hz.	Ensures accurate positioning of the FPA for in-focus captures	Demonstration
E.3.1	The feedback mechanism shall be calibrated through at least the full range of travel of the mechanism	This ensures the feedback is valid through the entire range of travel	Test
E.4.0	The focus mechanism shall not contribute electromechanical interference to the rest of the payload or bus	The solution cannot interfere with other space vehicle functionality	Demonstration
E.5.0	The focus mechanism shall respond to a command from the bus within 50ms	Low latency ensures agile mission response	Test

Table 5: Electrical System Requirements

3. Environmental

ID	Description	Rationale	Verification Method
ENV.1.0	All components of the focus mechanism shall have a survival temperature of at least -40C to 85C and an operational temperature of -20 to 60C	Anticipated environmental conditions for the mission	Test per GEVS
ENV.2.0	All materials shall be low outgassing as defined by a Total Mass Loss of less than or equal to 1.0% and a Collected Volatile Condensable Materials less than or equal to 0.1% when tested to ASTM E595. Allowances for low volume, low surface area materials or other material use cases may be approved on a case-by-case basis.	Anticipated environmental conditions for the mission	Test per GEVS
ENV.3.0	A safety factor of 1.25 on limit loads shall be used. If a component is qualified by analysis alone, a 2.0 safety factor on yield (2.6 for buckling) is appropriate to be used over limit loads. If qualified by analysis and test, the analysis will show a safety factor of 1.5 on yield (2.0 for buckling).	Ensure the survivability of the focus mechanism through launch	Test and analysis per GEVS
ENV.4.0	The system shall be subjected to random vibration tests in the X, Y and Z axes. Test tolerances will be ±3 dB on Power Spectral Density (PSD) spectral levels, and ±1 dB (true RMS) on the overall level for a duration of one minute, as shown in Figure ENV.4 below.	Ensure the survivability of the focus mechanism through launch	Test and analysis per GEVS
ENV.5.0	The system shall operate at 1e-5 torr vacuum and be compliant with ASTM E595 with a total mass loss of less than or equal to 1.0% by analysis.	Anticipated environmental conditions for the mission	Test per GEVS
ENV.6.0	Spacecraft hardware can be expected to encounter the radiation environment resident in a LEO polar orbit. Flight hardware is planned to be designed to withstand applicable environments. A strategy that combines metallic shielding as well as component selection for the space environment will be negotiated with LLNS.	Anticipated environmental conditions for the mission	Test and documentation

Table 6: Environmental System Requirements

Random Vibratin Test levels for Components ≤22.7 kg	
Frequency (Hz)	**Protoqualification ASD Level (g^2/Hz)**
20	0.026
20-50	+6dB per Oct
50-800	0.16
800-2000	-6dB per Oct
2000	0.026
Overall	**14.1 G_{RMS}**

Random Vibratin Test levels for Components 22.7 kg to 59.0 kg	
Peak Level (50 - 800 Hz)	=0.16*(22.7/Mass)
Slopes Maintained at + and - 6dB	

Random Vibratin Test levels for Components over 59.0 kg	
Frequency (Hz)	**Protoqualification ASD Level (g^2/Hz)**
20	0.01
20-50	Slope adjusted to match
50-800	0.16*(22.7/Mass)
800-2000	Slope adjusted to match
2000	0.01

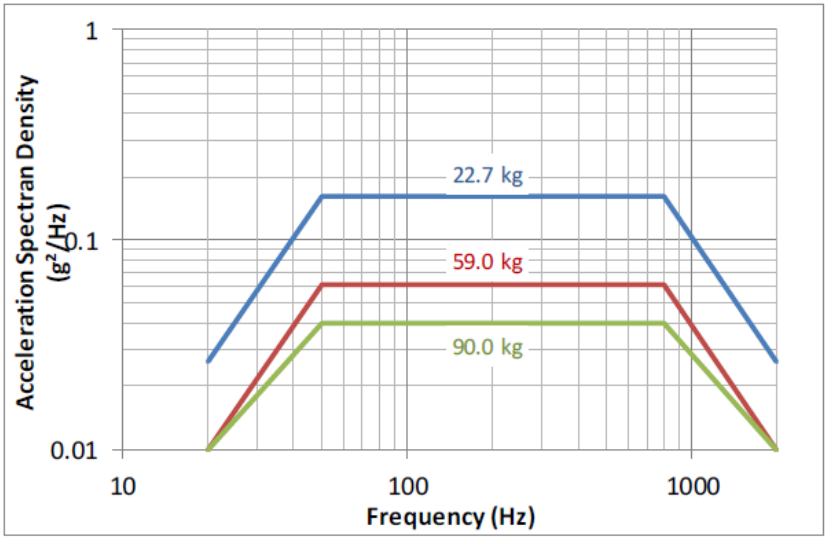

Figure 12: ENV4.0, random vibration testing conditions.

4. Safety

ID	Description	Rationale	Verification Method
S.1.0	The system shall not harm operator or assembly staff at any stage during development build or operation.	Required to meet LLNL management, launch partner and general public safety expectations.	Test and Demonstration
S.2.0	The system shall not in any way endanger the payload system during launch.	Required to meet LLNL management, launch partner safety expectations.	Test and Demonstration
S.3.0	The system shall not put affect the safety and operation of other low earth orbit scientific and defense platforms during operation.	Required to meet LLNL management, sponsor, and general public expectations.	Demonstration

Table 7: Safety System Requirements

III. Approach

A. Design

1. Mechanical

The focus mechanism consists of a linear actuator mechanically coupled to an image sensor. Figure 14 shows a cross section of the design. The actuator controls the placement of the image sensor along the optical axis. However, though the idea appears simple, careful mechanical design is required to provide the required performance. For the purpose of this thesis, the only elements of the mechanical design that will be analyzed are those that directly pertain to the electrical performance of the system. Those can be broken into two elements: axis isolation and actuator coupling.

Axis Isolation: A single axis stepper motor is employed for the focus mechanism. That means there is only a single degree of freedom (position along the optical axis). Therefore, the remaining five axes (two linear, three rotational) must be constrained to ensure system performance. This is accomplished by including a linear bearing parallel

to the optical axis. The bearing ensures translation along its axis while constraining additional movement. Figure 13 shows a single flexure. When displaced in the ±x direction, the flexure allows for translation. Any motion in the y or z axis are constrained. The focus mechanism uses two thin flexures, shown in green in Figure 14.

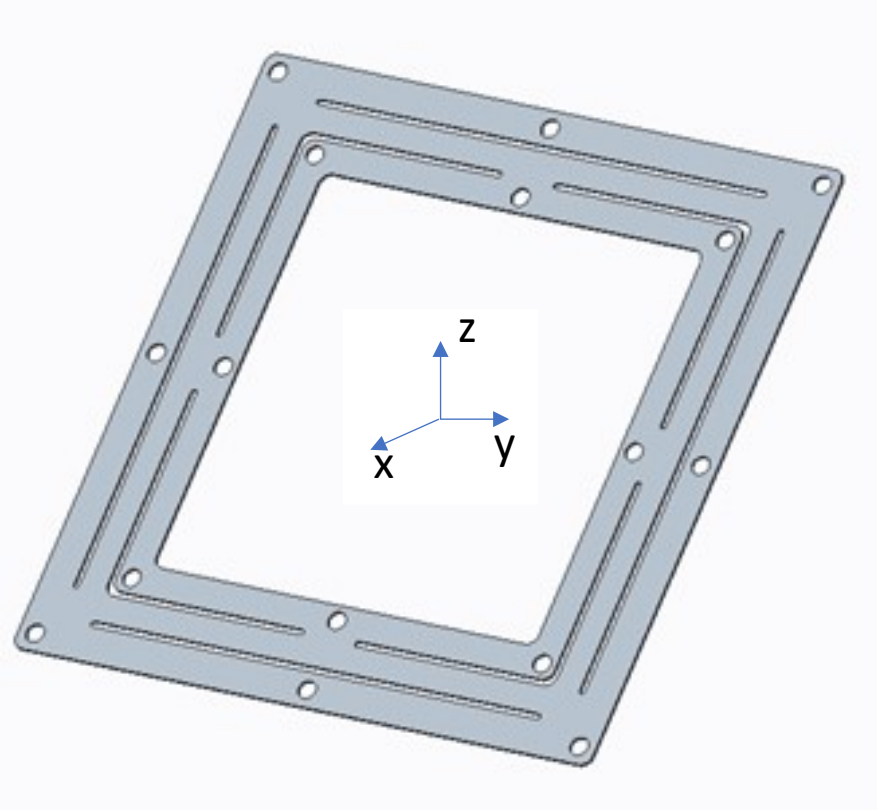

Figure 13: flexures employed in the focus mechanism to provide axial isolation.

Actuator Coupling:

How the actuator is coupled to the image sensor is largely determined by the axial load that the actuator is rated for. This is a consequence of extreme launch conditions. Without employing an additional mechanism to hold the image sensor in place during launch, the actuator (in an unpowered state) takes the load of the image sensor. For example, under 14Grms acceleration, with 3σ margin, an image sensor assembly weighing 500g exerts

over 200N of force on the actuator. Therefore, if the actuator is unable to withstand that amount of loading, mechanical advantage must be employed to reduce the perceived load. If the actuator is directly coupled to the image sensor, the configuration is called “direct drive”, because the actuator is directly driving the sensor. If the actuator is coupled to the image sensor through a lever arm, this is known as a “rocker arm”.

The focus mechanism employed the rocker arm approach for the first engineering unit. It provided an approximate 2:1 mechanical advantage. Using the example above, 200N force in a direct drive configuration becomes 100N in the rocker arm configuration. As an added benefit, the minimum displacement of the image sensor is reduced by a factor of two. As an example, if the actuator moves 5um, the image sensor will only move 2.5um. The consequence of this configuration is that the total range of travel is also reduced by 2. For an actuator that has 10mm of travel, the image sensor will only have 5mm range of travel.

Figure 14 shows a cross-sectional view of the mechanical design. It becomes clear that the camera (purple), is sandwiched between two-thin flexures (green), as described above. The camera housing (red) provides an easy interface with the rest of the system. The linear actuator (grey) is coupled to the camera housing through the rocker arm (orange). The rocker arm is the component that provides the mechanical advantage of the system. The rocker arm, actuator, and camera housing are held together in the out frame (blue). Note: a linear variable differential transformer (LVDT) displacement sensor can be seen mounting on the outer frame and making contact with the inner camera

housing. This sensor will be discussed in more detail in the following section. Figure 15 shows a 3D CAD representation of the final focus mechanism design.

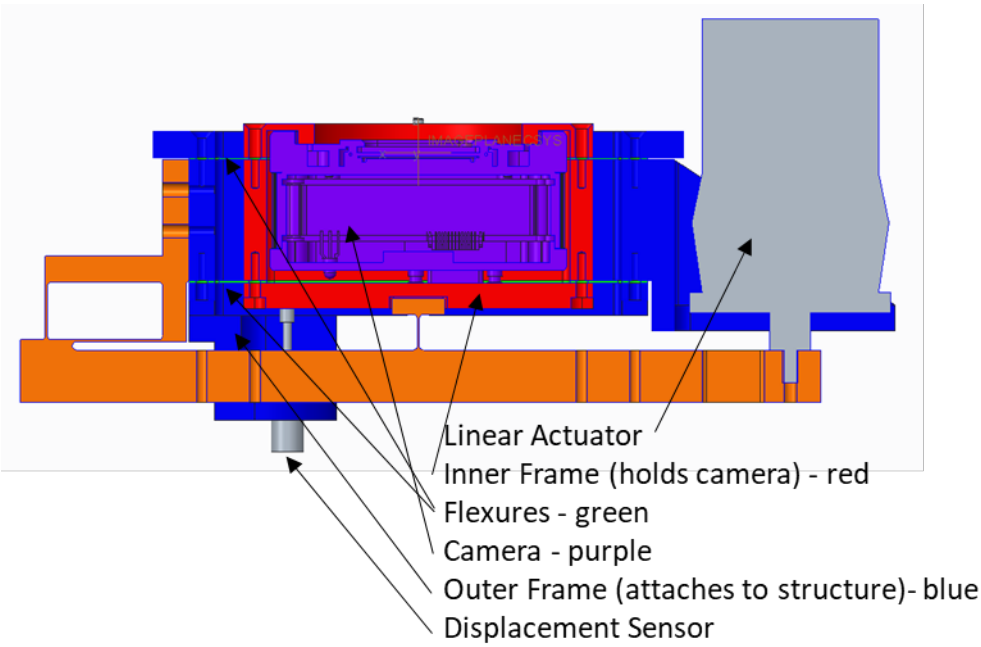

Figure 14: Section slice of the focus mechanism, showing key components.

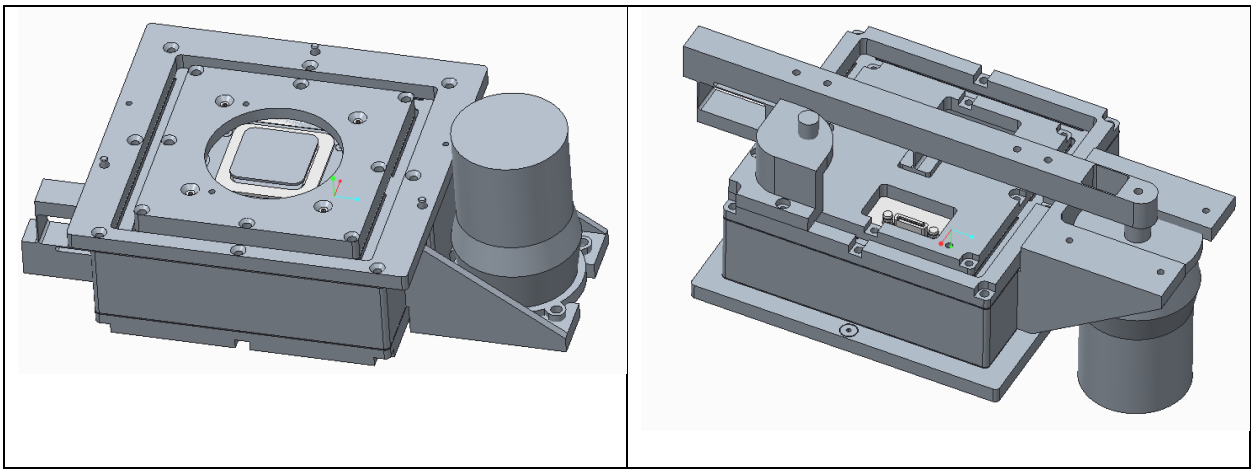

Figure 15: CAD representation of the focus mechanism.

2. Electrical

Actuator: A constant voltage stepper motor was chosen for the engineering unit. Constant voltage motors are simpler and lower cost to implement compared to their constant current counterparts. Due to the relatively low duty cycle and required motor speed, the decrease in torque at higher speeds, which is associated with constant voltage systems, was deemed insignificant.

Phytron, a German company, was selected to produce the actuator. Phytron is an industry leader at providing precision electromechanical solutions for extreme environmental conditions. Though the engineering unit was not intended for flight, a flight-like unit was procured in order to validate launch load conditions (discussed in the Section I.C.3 **Environmental Conditions**). This means the unit met the stringent requirements necessary for environmental testing. The engineering unit was specified as a slightly modified version of Phytron's "phySPACE" line of space-rated linear actuators.

The actuator is a bipolar 1.8°/step stepper, 24V/1.4A design, with a minimum full step linear translation of 5um. Due to the mechanical leverage of the rocker arm, the focus mechanism has an approximate 2:1 advantage ratio. A 5um delta at the actuator results in a 2.5um sensor adjustment. Additionally, the unit does support micro-stepping (1/2, 1/4, 1/8, 1/16, 1/32, 1/64, 1/128, and 1/256 steps). At 1/256 step, the theoretical limit to step displacement is roughly 10nm. This exceeds the mission requirements and measurement capability. As such, individual micro-steps were not employed as a method of translation. Additionally, for such small displacements, surface roughness of the lead

screw internal to the actuator would likely limit the practical minimum translation of the mechanism. The full step repeatability is examined in Section III.B.

Controller: though the actuator needed to be flight-like, the controller did not. This is because all environmental testing was performed at the subassembly level, as compared to an integrated payload. The controller (as well as the diagnostic and supporting electronics) will not be subjected to the same environmental testing as the actuator. As such, the Phytron MCC-1 was chosen as an off-the-shelf controller solution.

The controller supported single axis control, with either USB/Ethernet/RS-485/RS-232 interface (MCC-1, 2021). USB 2.0 was chosen for simplicity. The controller required a 24-48V single-power supply input. Depending on the intended use of the controller, both Phytron supported both a custom controller software (MiniLog-Comm) and publicly available LabVIEW Virtual Instruments (VI). Due to the simplicity of the environmental testing, MiniLog-Comm was sufficient to control the actuator and required reference performance tests.

Feedback Approach: The focus mechanism is designed to operate in open-loop control. That is to say, no feedback is required for the mechanism to support its primary objective of optical focus. This is in large part due to the reliability and repeatability of the selected actuator, as well as the deterministic nature of optical systems. Because the focus mechanism is primarily compensating for deltas induced by thermal expansion throughout the system, the required offset of the image plane is easily calculatable. Thermal

simulations will yield a look-up table that determines the required focus position based on current telescope temperatures. Additionally, the best focus for a particular distance to target is an easily calculatable parameter of an optical system. The theory of operation for the focus mechanism is discussed in more detail in the following sections.

While the focus mechanism can operate in open loop, the engineering unit was designed to support position feedback. The primary motivator of this was to provide easy reference data during testing. In the event that a mission requires position feedback (likely as a risk mitigation procedure), the focus mechanism could support this without redesign.

LVDT: a linear variable differential transformer (LVDT) was selected as the position feedback device for the device. The motivation for this was their robustness in extreme environments, coupled with easy implementation for terrestrial analysis. LVDTs require significant amounts of signal-conditioning to translate a linear mechanical displacement into a proportional DC electrical output. However, because the required signal-conditioning is off-sensor (i.e., in a controller), the reliability and repeatability of an LVDT was extremely desirable.

LORD Microstrain was selected as the vendor for the LVDT. An off-the-shelf non-contact LVDT with 4mm stroke was chosen, paired with the LORD DEMOD-DVRT-2 signal conditioner. The sensor has a full-scale resolution of 8um, significantly lower than the required 30um minimum displacement of the focus mechanism. The signal conditioner required 12V DC input and produced an analog output (0 – 12VDC). The output signal

needed to be recorded and translated to linear positioning using the calibrated reference documentation from LORD.

Image Sensor: There are innumerable variables that play a role in determining the sensor for an optical system, as discussed previously. For simplicity, an off-the-shelf sensor and frame grabber were chosen for the focus mechanism engineering unit.

The sensor selected was the On Semiconductor Python NOIP1xx025KA CMOS imager. In addition to peak quantum efficiency of 50%, the detector has a native resolution of 5120 x 5120 pixels (4.5um/side) and can support up to 32 frames per second in global shutter. The diagonal of sensor is roughly 32.5mm, allowing it to support an impressively large exit pupil of an optical system. Imperx, an industrial camera and imaging company, provides a ruggedized series of cameras known as Cheetah. The Cheetah C5180-CLF packages the Phyton sensor, along with a proprietary frame-grabbing FPGA, in a robust mechanical structure that features a CameraLink-Full (CLF) imaging interface.

Though CLF provides superior optical performance and throughput, it is more challenging to interface with than alternatives (such as USB or GBE). Specialty PCIE cards are required to interface with a CLF camera directly. However, there are converters which allow a user to use more common communication protocols. Pleora is a Canadian company that provides a broad range of imaging solutions. The iPORT CL-U3 was procured to support field-testing of the C5180. This frame grabbing peripheral allows interface with CLF cameras over USB 3.0.

3. Theory of Operation

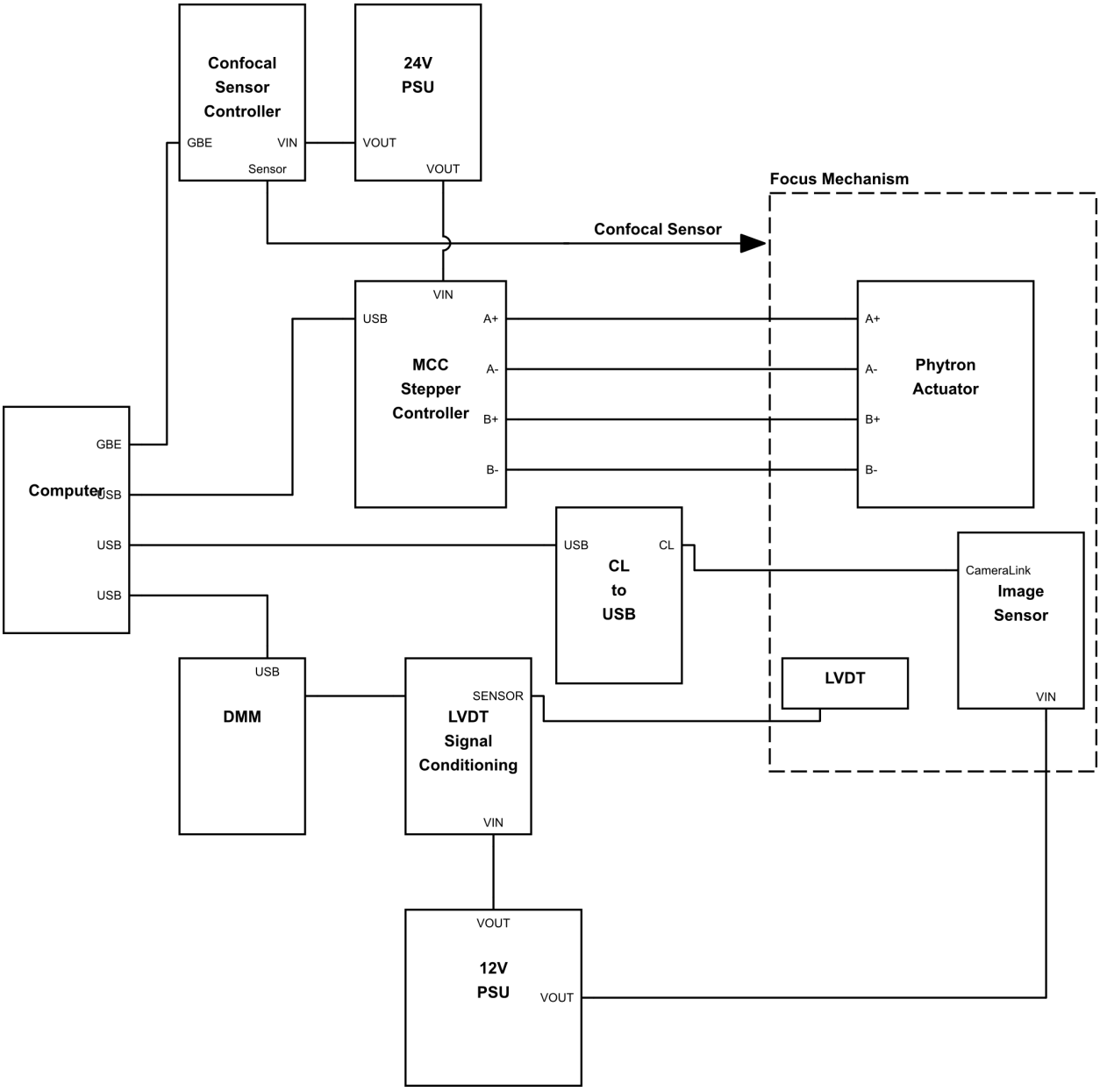

Figure 16: Block diagram of the focus mechanism control and operation architecture.

The above diagram graphically displays the theory of operation for the engineering unit focus mechanism. The dashed line represents the engineering unit focus mechanism

assembly. All other boxes are support and/or diagnostic equipment that are not intended to be considered part of the design.

Power supplies (PSU): power using benchtop power supplies for the required 12 and 28V lines. These supplies will provide current limiting to ensure circuit protection in the event of an anomalous event.

Position feedback: the analog output of the LVDT signal conditioner is logged using a benchtop digital multimeter (DMM). While the voltage reference can be read in real-time, the position translation takes place by post-processing the data in MATLAB.

System Control: for the purposes of the engineering unit, a laptop computer takes the place of a payload controller. The laptop interfaces with the MCC-1 motor controller over USB. There is no payload controller emulator; the MCC-1 receives commands from the laptop ad-hoc in real time. Similarly, the camera is controlled by the laptop (via the CL-U3 adapter).

B. Calibration

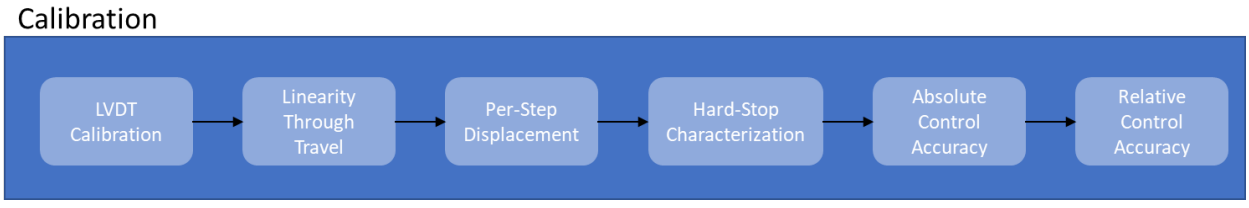

Figure 17: Calibration Sequence Flow Diagram

Figure 17, above, shows the flow of the calibration activities that were executed prior to environmental testing.

1. LVDT Recalibration:

In order to support thermal-vacuum (TVAC) testing, certain cables needed to be spliced through the bulkhead connector. As it was impractical to have a DMM reside inside of the TVAC chamber, the LVDT cable from sensor -> demodulator needed to be cut. Splicing this cable to a bulkhead connector significantly changed the electrical characteristics of the sensor. Prior to environmental testing, it was discovered the LVDT needed to be recalibrated from its manufacturer reference. This was accomplished using a Mitutoyo Series 521 Calibration Tester. The 521 is an analog gearing system, capable of sub-300nm displacement, with a 1.27mm range. The non-contact LVDT sensor was connected to the translation stage of the 521 and taken through the sensor's full 4mm range of travel, with four overlapping datasets. For example, consider the Z-axis as the displacement axis. The first dataset had the LVDT start at Z = 0. The 521 was taken through its full 1.27mm range, ending at Z = 1.27. The 521 was then reset for a second dataset. However, the LVDT was not reset. Instead of the LVDT beginning at Z = 0, it now began at Z = 1.27. This process was completed four times. The demodulated analog output was measured translated to linear position, using the 521 as reference truth. Figure 19, below, compares the recalibrated LVDT data with the initial manufacturer measurement.

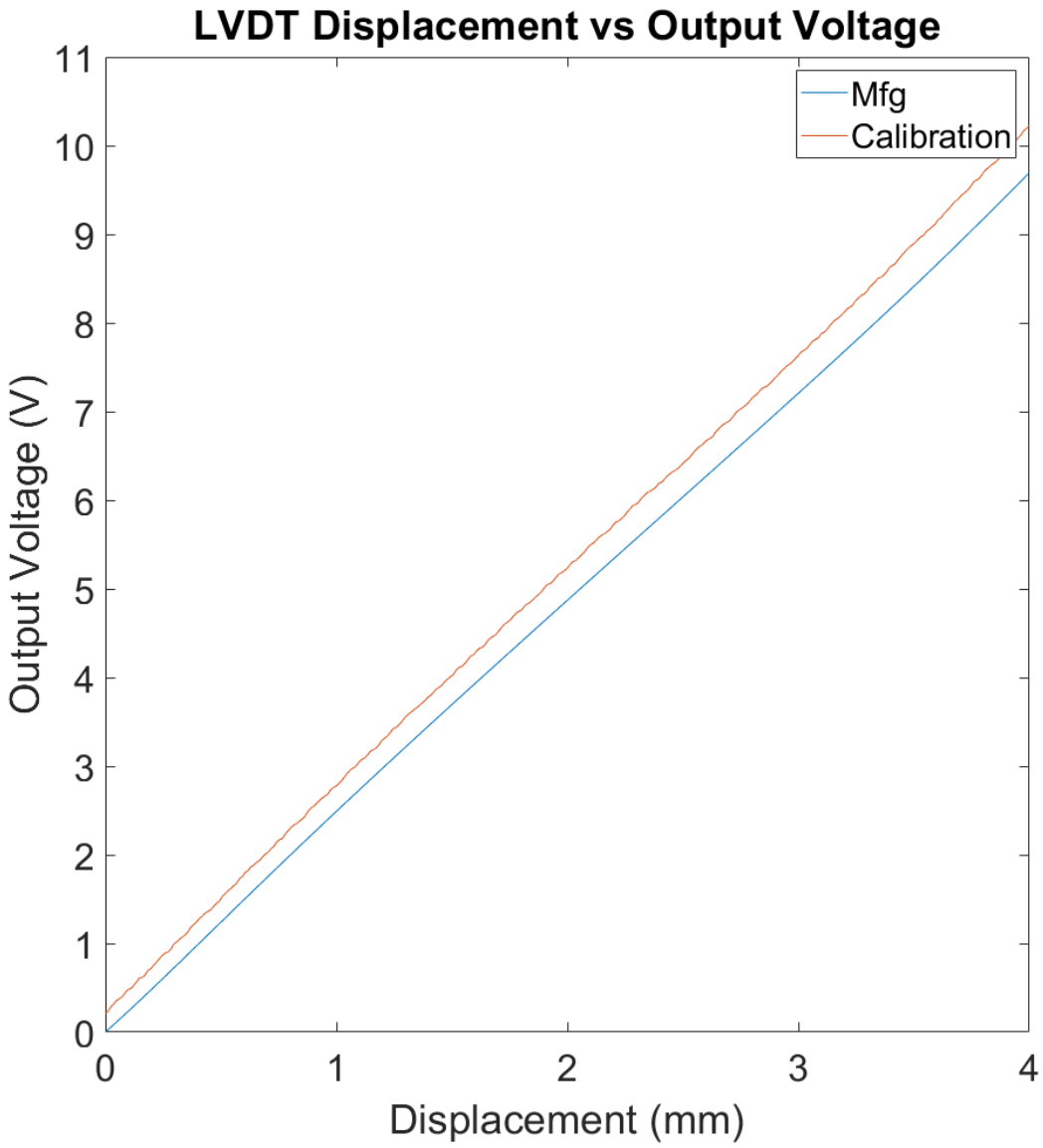

Figure 18: Comparison of the manufacturer calibration dataset (Mfg) with the recalibration (Calibration) dataset. There exists an approximate 375um constant offset between the two datasets.

2. Focus Mechanism Performance Test Setup:

The focus mechanism was assembled and configured, as described in the previous section (block diagram shown in Figure 19). Prior to environmental testing, the following important metrics of the system were characterized: linearity of steps through the full

range of travel, average step size across the range of travel, overdriving at a hard-stop, and desired vs measured position.

Though the focus mechanism supported LVDT feedback, the position data for these tests was taken using confocal interferometry. The confocal interferometric displacement measurement is impractical for orbital measurements but ideal for laboratory performance testing, as it offers superb resolution and accuracy (sub 10nm). The confocal spot was focused on the moving mass of the focus mechanism (the inner frame, as shown in red in Figure 14 not the actuator itself. Though displacement characteristic of the motor itself could be of academic interest, the more concerning metric is the behavior of the camera internal to the focus mechanism.

All the above tests were taken under the same testing conditions and testing set up. The focus mechanism and confocal sensor were secured to an air-insulated optical table to minimize vibrations. All other supporting equipment was placed on an adjacent work bench.

Equipment:

- Tektronix 2280S-32-6 PSU at 24V/1A limit
- Tektronix DMM7510 with 10kS/s, 5s windowing, 6.5 significant figures, and 1A limit
- Micro-Epsilon confocalDT 2422 with 1mm and 10mm optics
- Phytron MCC-1 motor controller
- Thorlabs optical table
- PC with MATLAB

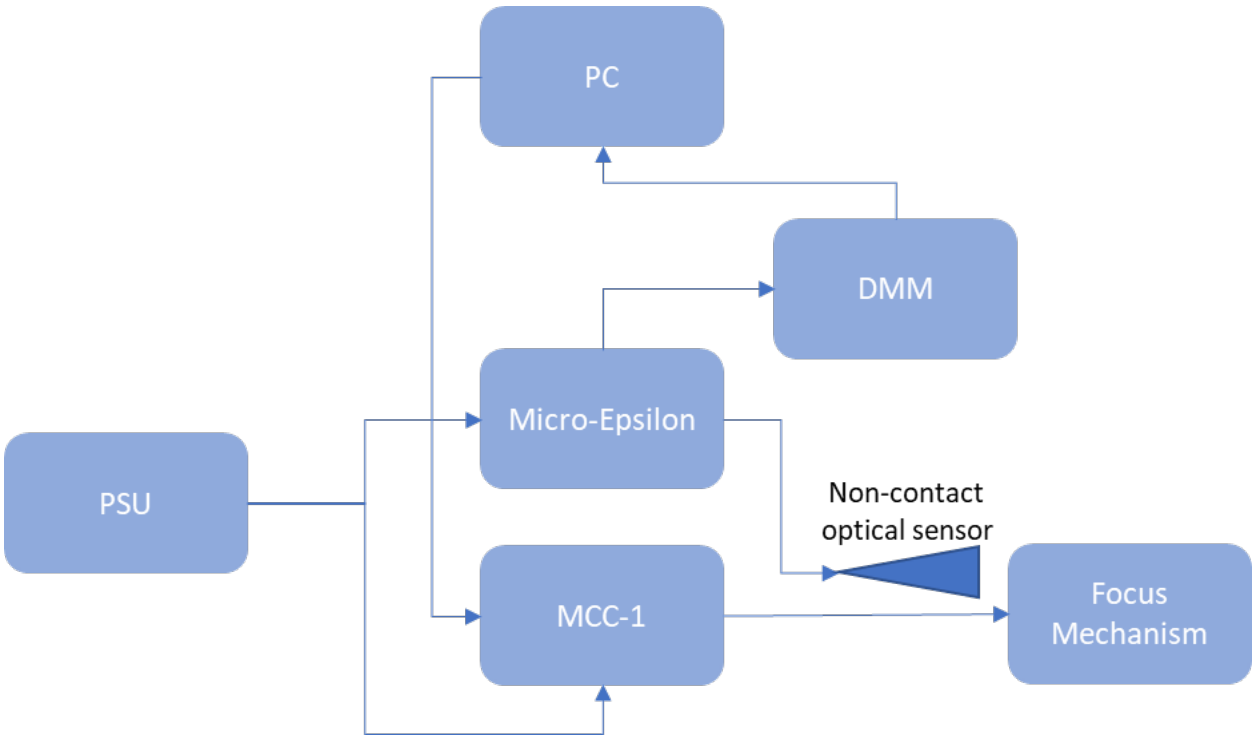

Figure 19: Calibration Test Setup

3. Linearity of Steps Through Full Range of Travel:

The goal of this experiment was to measure the linearity of the focus mechanism through its full range of travel, which is approximately 1000 steps. This measurement is extremely important for operating the device in open loop. If the mechanism shows linear behavior throughout the range of travel, then a lookup table may not be required. If, however, the mechanism shows non-linear behavior, it is important to accurately characterize this to account for it when sending displacement commands.

The test was repeated four times: three times with a 1mm confocal sensor and once with a 10mm sensor. The 1mm had significantly higher resolution (below 10nm) but could not measure the focus mechanism through the full range of travel. The 10mm sensor, on the other hand, had noticeably lower resolution (and increased noise) but could measure the

mechanism through its full range of travel. In order to take measurements with the 1mm sensor, the actuator would go through 1mm of travel, the sensor position would be reset, and the actuator would go through another 1mm displacement. This process was repeated through the full range of travel, with slightly overlapping datasets.

As can be seen from Figure 20, below, the focus mechanism showed very high repeatability through its full range of travel. The three datasets using the 1mm sensor agree to within 1um, and the lower resolution 10mm sensor exhibits the same behavior as the 1mm. Noticeably, there are two significant bumps that occur from 400 to 650 steps. Due to the nonlinear behavior observed during test, a look up table would be required for operation on orbit. The noise shown on the “lower resolution” dataset is an artifact and a remnant of the less precise 10mm sensor.

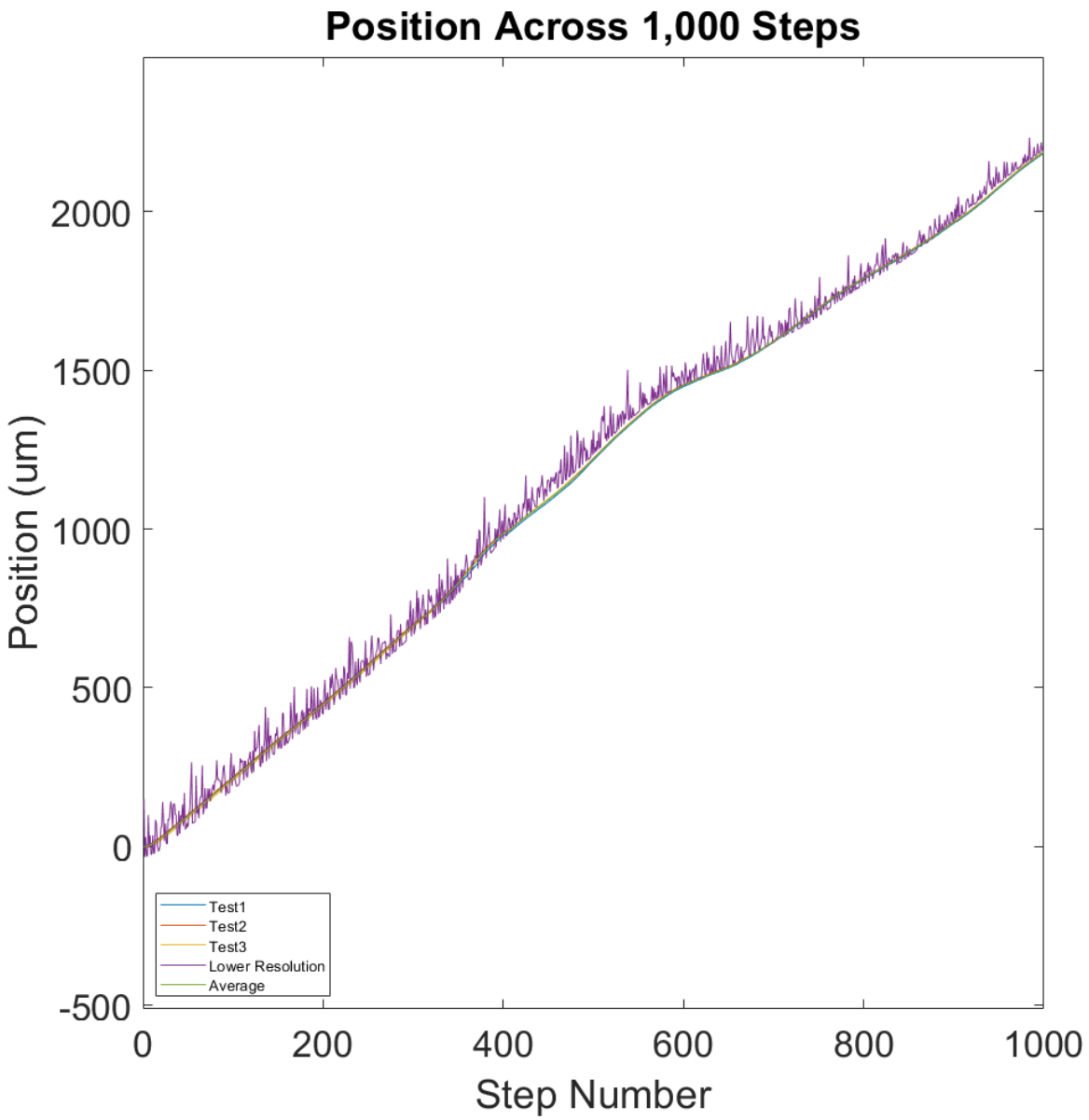

Figure 20: position of focus mechanism through full range of travel of the actuator. Step 0 and 1000 represent the physical hard-stops of the system.

4. Average Step Size

The step size is the derivative of the position vs step graph shown previously $\left(\frac{\Delta\ Position}{\Delta\ Step}\right)$. It is of interest to examine this directly. While controlling the absolute position of the focus mechanism is of interest, knowledge of its per-step displacement is also very important.

Consider an auto-focus routine, where an image is taken at each step. It is important to know what the displacement is between each image, in order to ensure accurate analysis.

Due to machine tolerances and nonlinearity of force applied through the flexures, it is not expected to measure identical steps at the focus mechanism, even though the actuator should produce nearly identical steps. Large deviations (> 5um) would indicate issues with either the motor or the flexures in the focus mechanism. Figure 21, below, shows the per-step displacement across the full range of travel. Similar to before, the test was repeated three times with the 1mm sensor. In the Test 1 dataset, there is an abnormally large step at 375. This behavior was not repeated in Tests 2 or 3 and is considered to be an outlier. While the data is repeatable, there is over a 3um change in per-step displacement. If the focus mechanism is to operate in open loop, a lookup table would be required for operation on orbit to ensure accurate position knowledge.

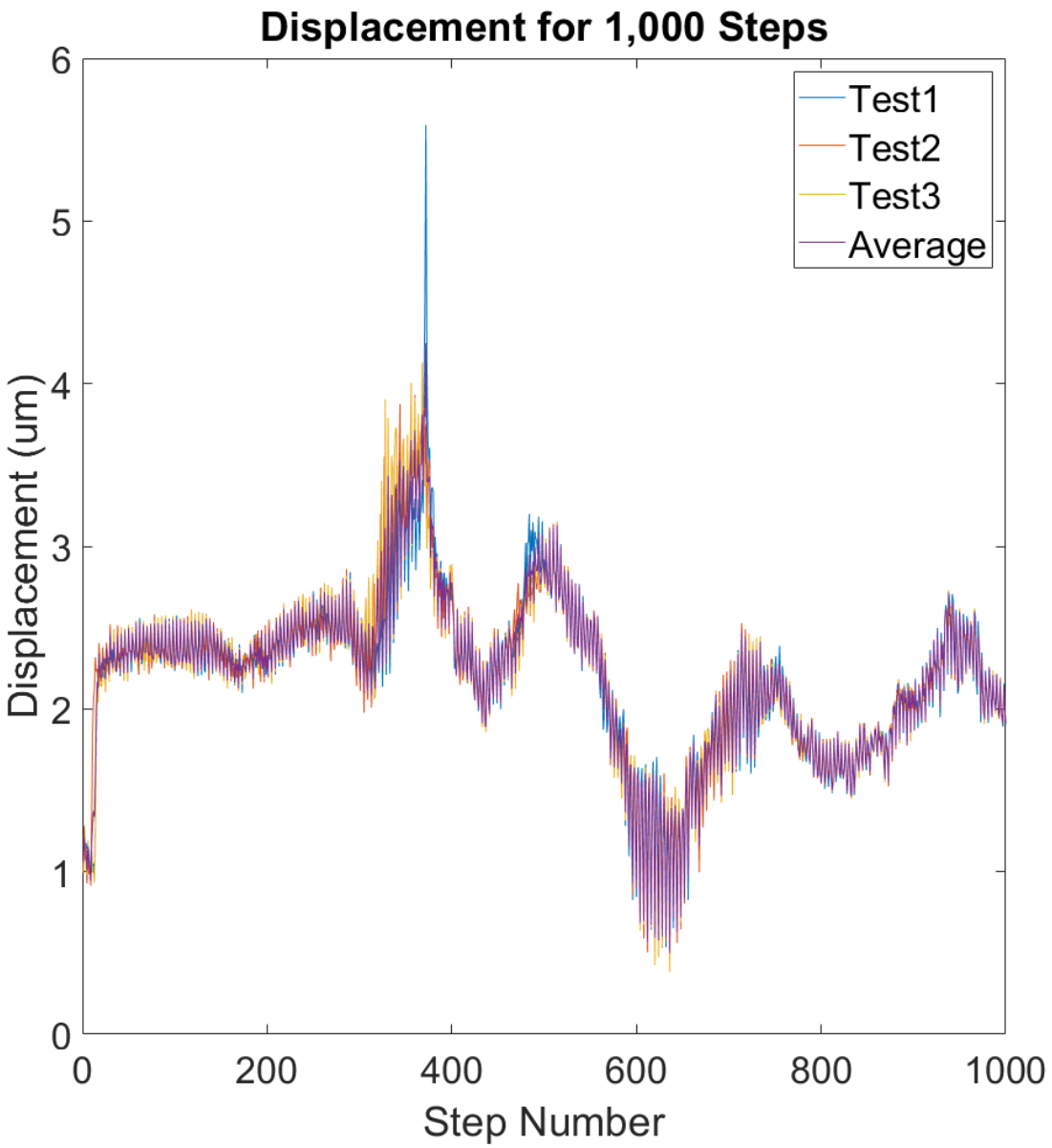

Figure 21: This figure shows the per-step displacement across the full range of mechanical travel for the actuator. This test was taken using the 1mm optic on the confocal sensor.

5. Homing to a Hard Stop

An important component for operating the focus mechanism in open loop is the ability to drive to a known reference position. This is commonly referred to as a hard-stop: a

position a motor can return to and be confident it hasn't driven past. Driving to a hard stop is a viable strategy for stepper motors, as attempting to drive the motor against a physical block, for a short period of time, will not result in damage to the motor. The motor will apply as much torque as it is rated for, and the stator will "slip" a step. However, even though no damage will come to the motor for a short-duration home routine, the stalling stator cycle will cause some amount of back-and-forth movement against the hard stop. Therefore, it is important to characterize the maximum average slippage from home that overdriving causes the motor. Homing to a hard-stop in open loop is only viable if the uncertainty associated with this strategy is much smaller than the precision requirements of the system.

The following test drove the motor to a hard stop, and then continued to overdrive the motor against that hard stop in single step increments. The confocal sensor measured the displacement caused by overdriving against the homing hard stop. The test showed that the maximum displacement in over-driving at a hard stop was less than 1.5um but varied significantly from step-to-step. For the precision required for the focus mechanism, this is an acceptable amount of uncertainty at the home position. The hard stop represents the only way for the motor to return to a known position, while operating in open loop. Therefore, variance in over-driving at a hard stop is the minimum uncertainty that will exist in the system. For any missions or optics that required greater precision than 1.5um, it is likely that closed loop feedback would be required.

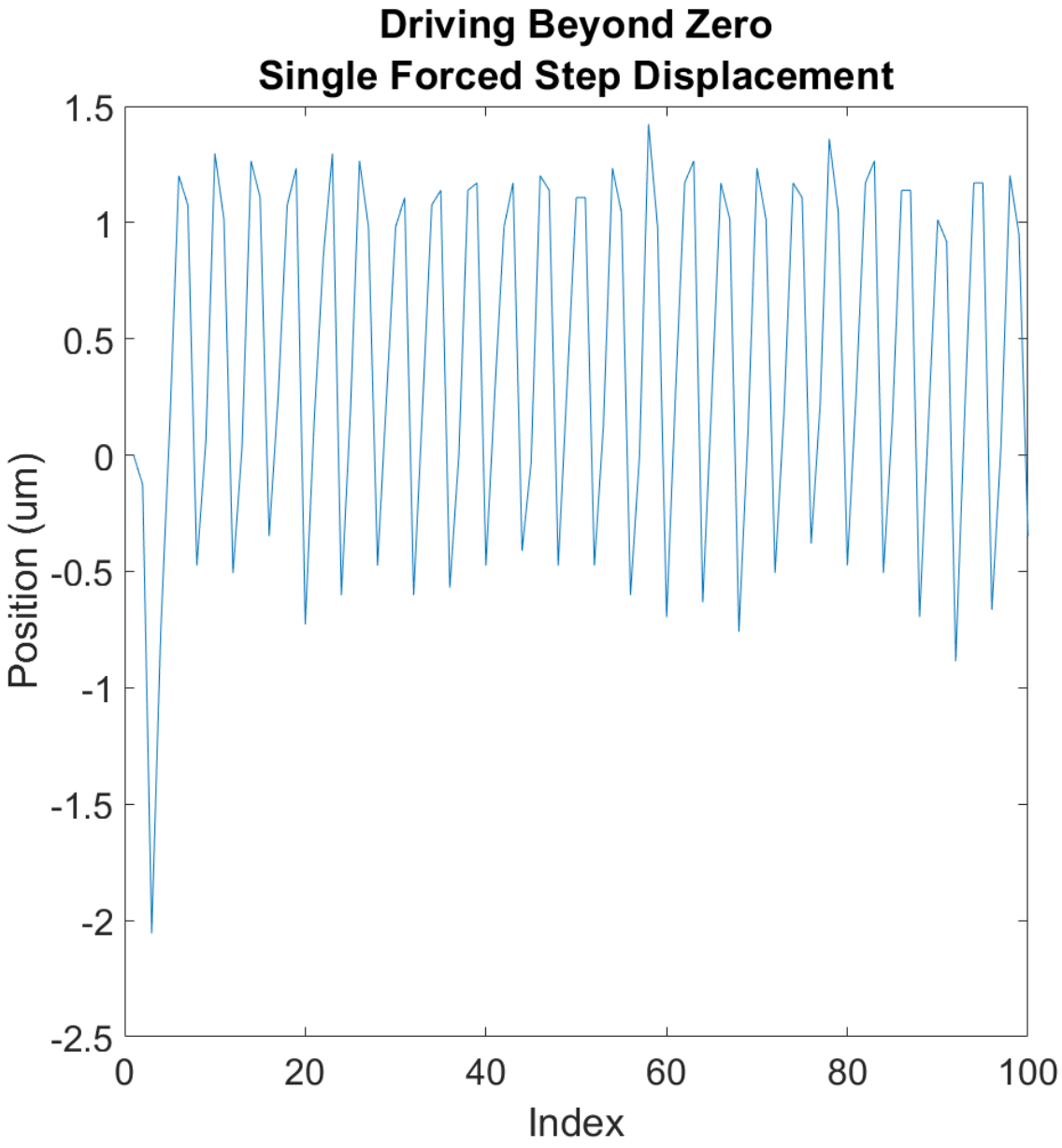

Figure 22: The actuator was driven against the negative hard stop in single step increments 100 times. Each time, the deflection from start was measured.

6. Desired vs Measured Position

Perhaps the most important initial test of the focus mechanism, from an electrical control perspective, is the difference between commanded position and actual position. So long

as this difference is significantly smaller than the required precision, the mechanism is shown to be operating successfully in open loop. When a specific location is requested (i.e., +75um or -25um), that command must be executed as a number of steps; the control takes commands in units of steps, not position. Therefore, the actuator was set to step through its full range of motion in increments of 30um (the minimum expected required displacement).

Two methods of command were used: absolute control and relative control. In absolute control, the actuator was driven to the hard stop and the step counter was set to zero. From there, a command would be executed (i.e., +13 steps), then a follow-on command would send the motor back the same number of steps (i.e., -13). The step counter was not zeroed between displacements. Contrary to this, in relative control, the actuator was driven back to its perceived home position, then it was driven several steps against a hard stop, ensuring it was as close to home as possible (with allowance for the slop in driving against a hard stop).

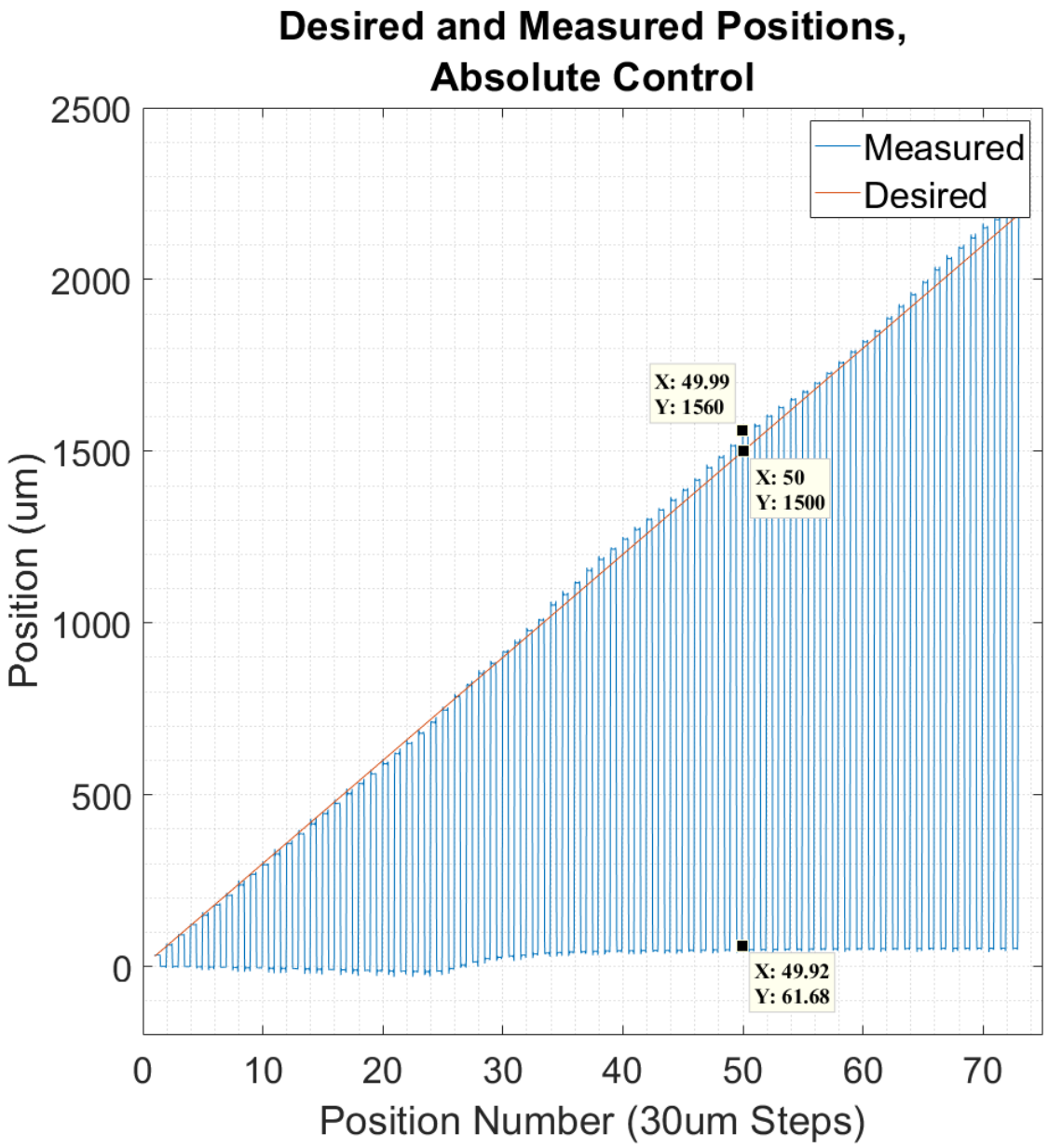

Figure 23: The focus mechanism was taken through its complete range of travel in 30um command increments.

Absolute control showed there was a difference of approximately 60um between measured and desired position. This difference began to become pronounced at position number 26 (corresponding to 780um) and was present, to varying magnitudes, throughout the remainder of the test. However, at this exact position, a noticeable ground-

difference appears of approximately equal magnitude. The figure above shows that at position 50 (1500um), there is a 60um difference between measured and desired positions. There is also a 61um difference between initial zero position and the current position. The difference between measured and desired positions is significant for the focus mechanism and exceeds its accuracy targets. Therefore, further testing and characterization would be required to fully diagnose the source of the discrepancy. If taken in isolation, a 60um uncertainty is unacceptable and would mean the focus mechanism could not operate in open loop. However, while this test was only performed once, the per-step displacement and linearity through range of motion (shown previously) were tested multiple times. Those tests showed high repeatability, indicating it is likely that the maximum 60um uncertainty is also repeatable. If the uncertainty is repeatable, it could be compensated for with a look up table.

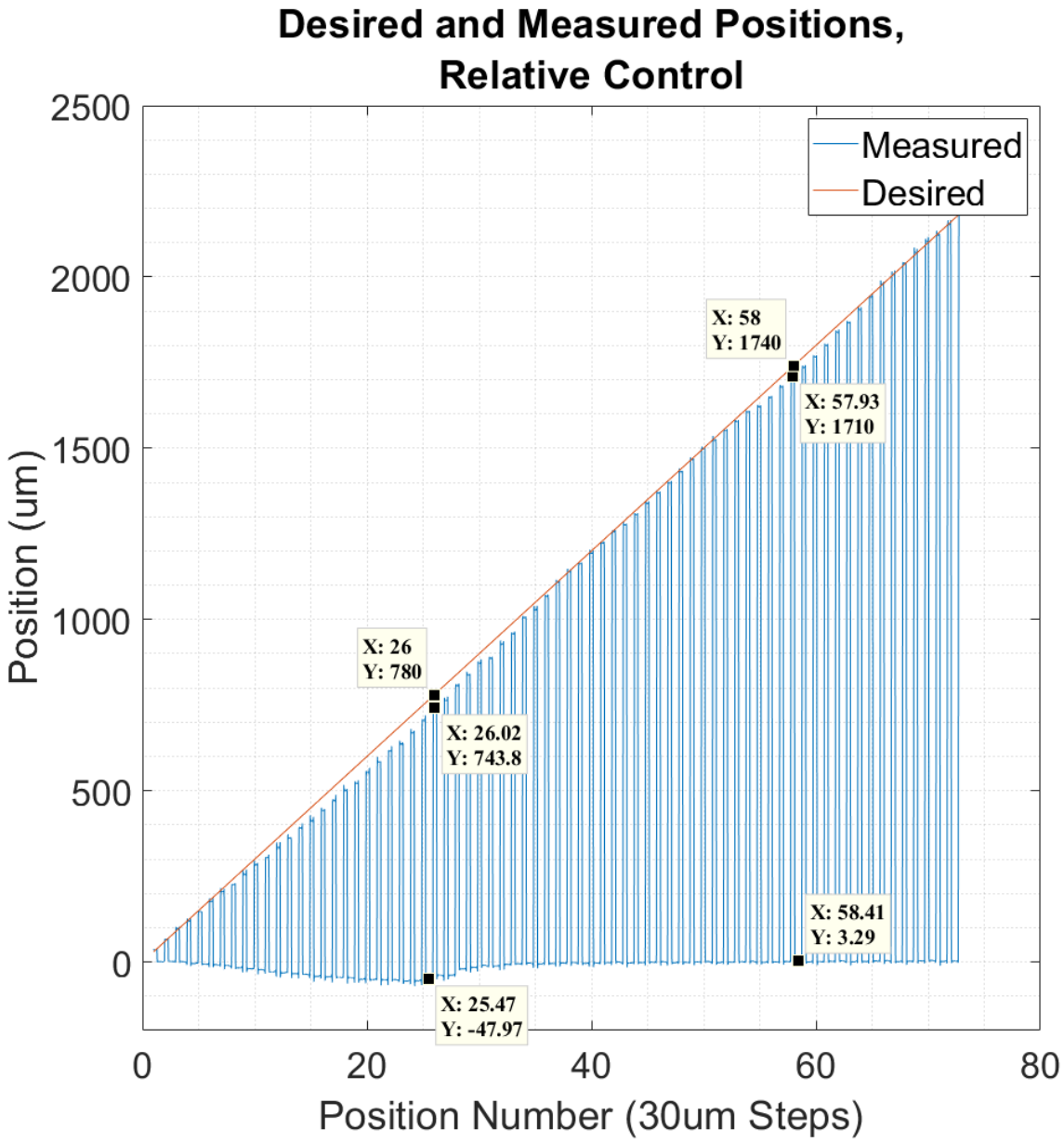

Figure 24: The focus mechanism was taken through its complete range of travel, in command increments of 30um, with a relative control scheme.

The relative control scheme exhibits very similar behavior as the absolute control scheme. The initial zero position drifts from 0um to almost -50um by position 26 (780um). At this same position number, the difference between measured and desired positions is approximately 36.2um. After position 26, the zero position returns to approximately 0um

for the remainder of the test. The impact to the focus mechanism system overall is the same as discussed in the “Absolute Control” test. It is troubling that the absolute and relative control tests yielded different uncertainty values. Further investigation would be required to determine the root cause of both the uncertainty and the difference in control schemes. Theoretically, both control method should yield results to within the uncertainty of the hard-stop position (<1.5um in this case).

C. Environmental Testing

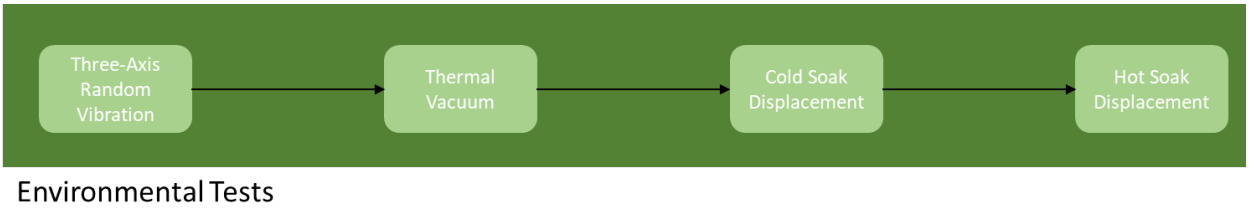

Figure 25: Environmental Test Sequence Flow Diagram

After initial reference performance measurements were taken, the unit was transported to an offsite facility to undergo environmental testing (Figure 25). This testing consisted of two stages: random vibration (vibe) and thermal vacuum (TVAC), according to GEVS Sections 2.4 and 2.6, respectively (GSFC-STD-7000, 2019). As this was an engineering unit, the primary concern of environmental testing was whether or not the FPA electronics and the actuator would survive the test. Less attention was given to the mechanical enclosure (specifically, the flexures), as it was known there were likely going to be significant design modifications prior to the flight unit. As such, the criterion for success of environmental testing was pass/fail for clear damage. A pass for the electronics was providing baseline functionality after testing. A failure would be inability to communicate with or control any of the subsystems. Similarly, a pass for the mechanical design was an

intact focus mechanism. A failure would be visible damage to the mechanism. The following section examines the testing conditions, input profiles, and test results.

1. Vibe Equipment

Vibe testing is conducted in an off-powered state, as there are no components required to be energized during launch. Therefore, the only equipment required was a vibration table capable of providing the input excitation. A Unholtz Dickie RTS-5 electro-dynamic shaker table was used for this test. Additionally, the testing vendor provided three accelerometers for control, and five accelerometers were for analysis. The three control accelerometers were placed on the base plate (one for each axis). The five analysis accelerometers were placed as follows: two near the image sensor as additional control references, one near the face of the motor body, one on top of the camera housing, and one on the rocker arm directly behind the sprung mass.

2. Vibe Testing

The testing profile shown in Figure 12 was used as the input excitation. Before a primary axis was subjected to the provided test profile, a low-level random (LLR) sinusoidal sweep was performed in the same axis. After the initial LLR, the vibe profile was tested. After the primary excitation, a second LLR was performed. The LLR measurements are used as a reference to determine if the response had changed due to the primary test. In between testing each axis, the unit was physically examined for any noticeable damage. No reference performance testing was performed during vibe testing.

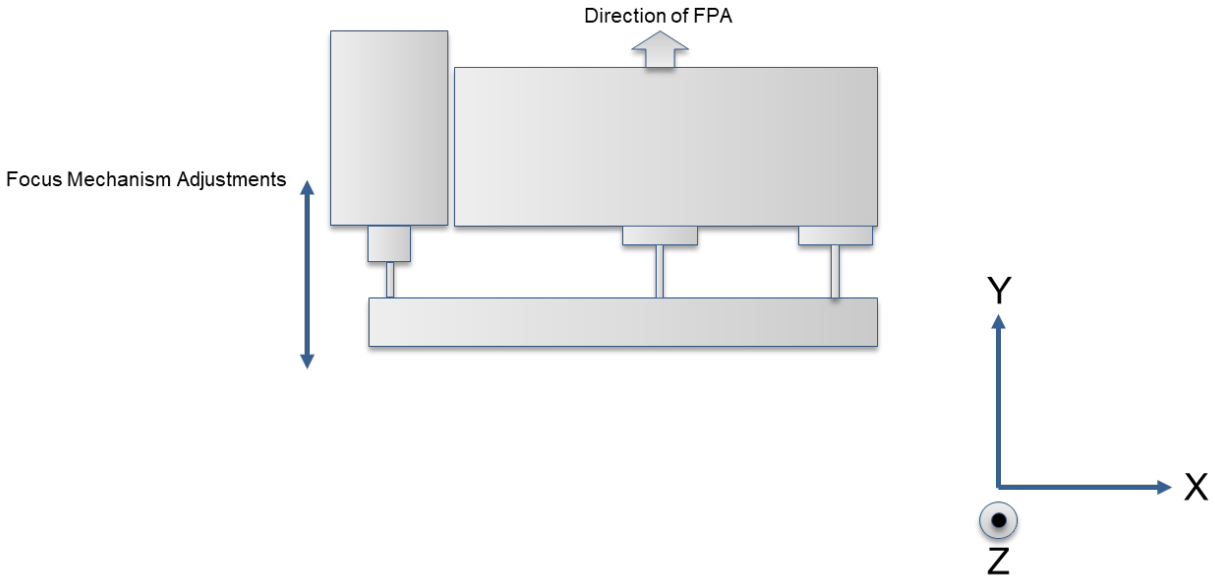

Figure 26: focus mechanism axis orientation definitions for environmental testing.

3. TVAC Equipment

- Abbess Instruments 363630-CHIL Thermal Vacuum Chamber
- Tektronix 2280S-32-6 PSU at 24V/1A limit
- Tektronix DMM7510 with 10kS/s, 5s windowing, 6.5 significant figures, and 1A limit
- Pleora CL-U3
- Phytron MCC-1 motor controller
- PC with MATLAB

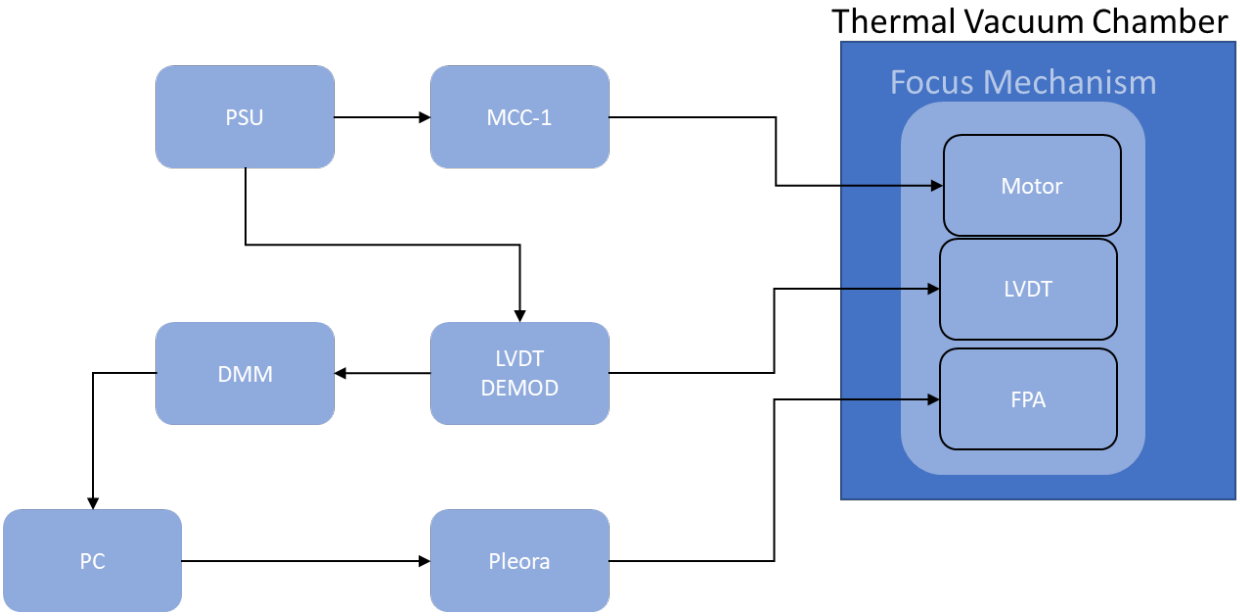

Figure 27: TVAC Block Diagram

In addition to the test equipment described above, the vendor provided several thermocouple channels that were used to monitor the control temperature of the chamber. Four thermocouples were used to monitor the focus mechanism: camera mount, top of camera body, the flexure arm, and the motor body.

Cable Feedthrough:

Figure 29 shows the required wiring diagram for the TVAC testing. A standard access port was provided by the testing facility. A custom 25-pin d-sub interface flange was created for the test.

As can be seen on the Figure 29, in addition to a 25-pin feedthrough, two CameraLink feedthroughs are required. This is to allow framegrabbing from the image sensor while under test. Due to the strict requirements of the CameraLink specification (as well as the total necessary pin-count), it was not possible to feedthrough these signals on a standard D-sub connector. Therefore, a custom interface board was designed and fabricated. Two of these interface boards were used to bring the required cables through the vacuum chamber.

The board was a very simple design. All it consisted of was two standard CameraLink MDR 26-pin connectors and a section of PCB. This PCB was fed through a bulkhead interface and epoxied in place using 3M 2216. The epoxy provided the required structural support, as well as a vacuum-strong seal.

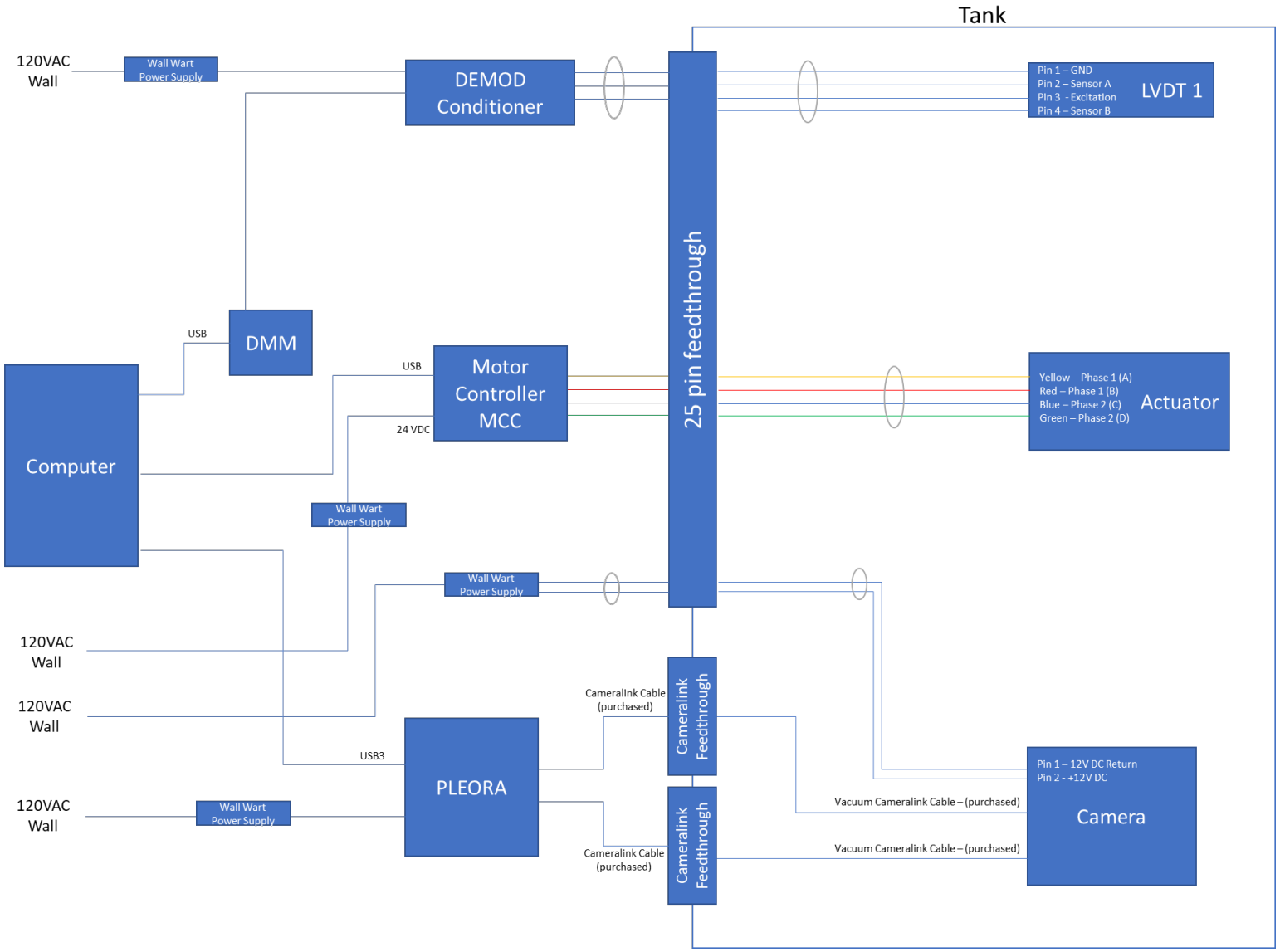

Figure 28: Wiring diagram for TVAC chamber bulkhead feedthroughs.

Figure 29: 25-pin D-Sub interface flange for the TVAC chamber.

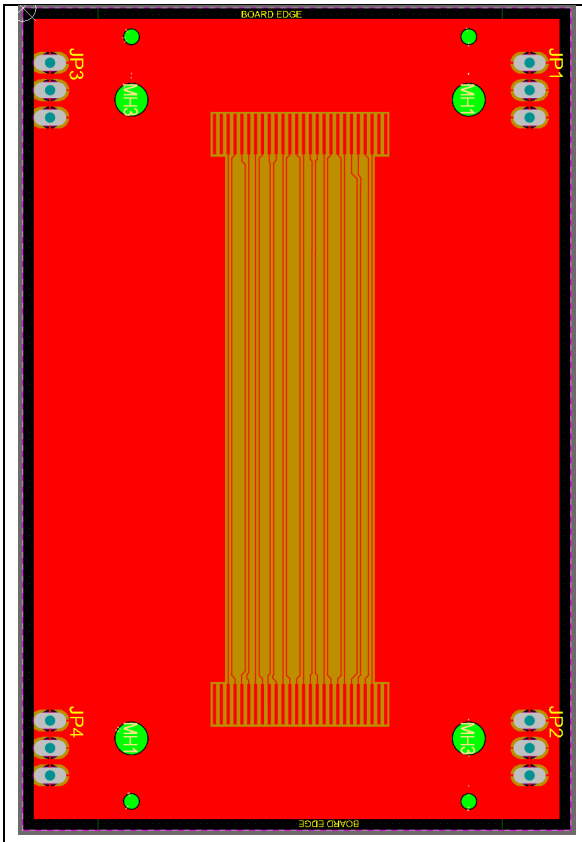

i.) PCB layout for the CameraLink MDR interface, created in Altium Design.

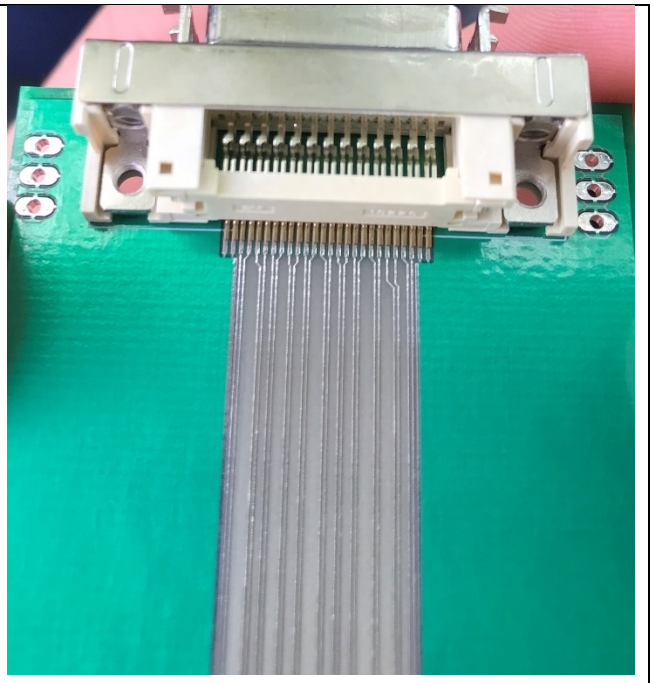

ii.) Picture showing one side of the fabricated and assembled PCB.

Figure 30: CameraLink interface PCB for vacuum testing.

4. TVAC Testing

Figure 31, below, shows the target test profile for the temperature sweep, with a goal pressure of < 1E-5 Torr (GSFC-STD-7000, 2019). Operational temperatures were specified as -40 to 60C. Because the focus mechanism was simply a subassembly of a larger payload, there was no hot or cold survival test. Instead, this period served as an additional soak at acceptance temperatures. It took the vacuum chamber approximately five days to pump down to below acceptance levels (1E-5 Torr, GEVS 2.6 (GSFC-STD-7000, 2019)). During the pump down time, the chamber temperature was held at maximum 60C to aid in volatiles outgassing more quickly. The duration it took the chamber to pump down to acceptable pressure is normal for this sort of operation. The time it takes to pump down is largely dependent on the cleanliness of the chamber and the device under test, as well as the power of the vacuum pump.

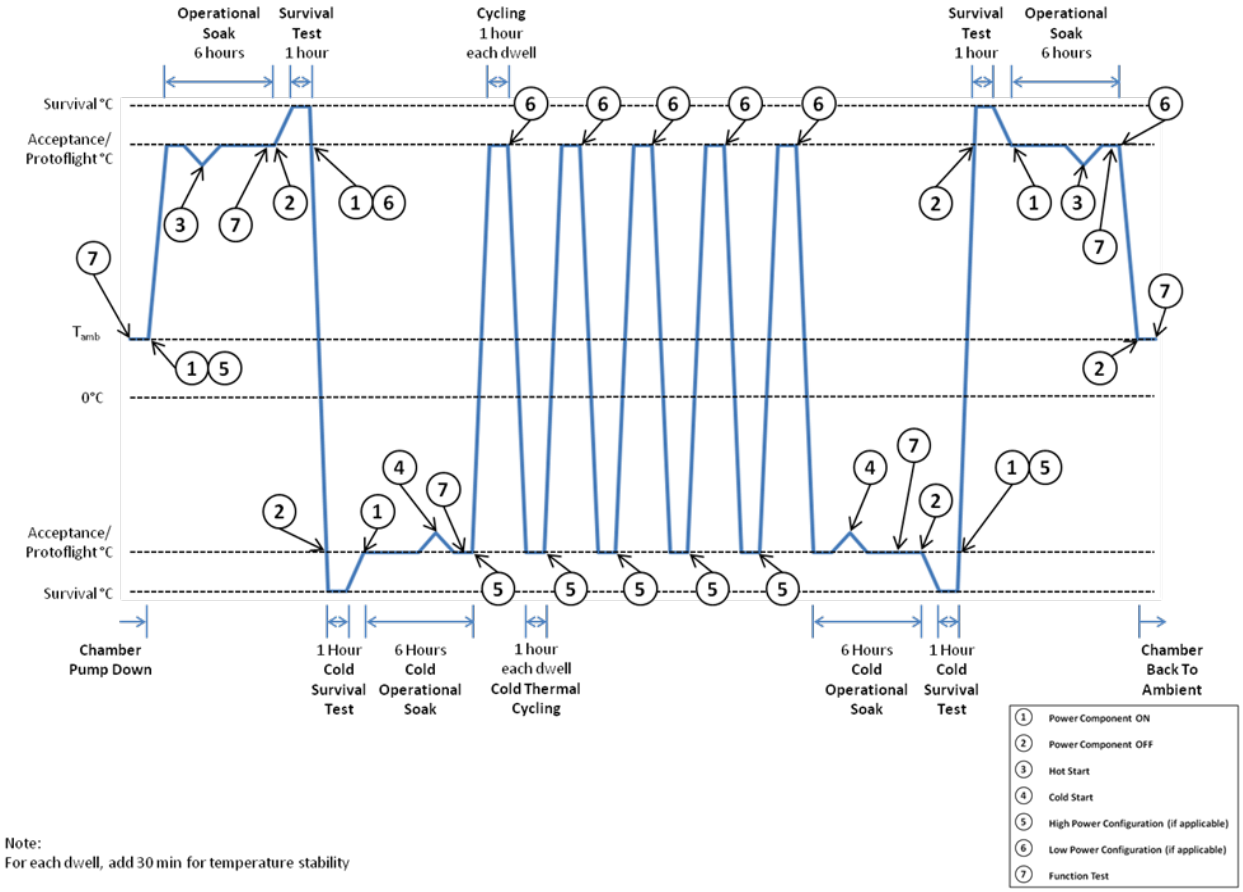

Figure 31: Thermal vacuum testing profile for the focus mechanism. Acceptance/protoflight levels were -40 to 60C.

IV. Results and Discussion

A. Vibration

1. Test Setup

The following images show the focus mechanism mounted to the vibration table and the placement of the accelerometers. The accelerometers were provided by the test provider to monitor the structural response of the system.

i.) Front side of the focus mechanism

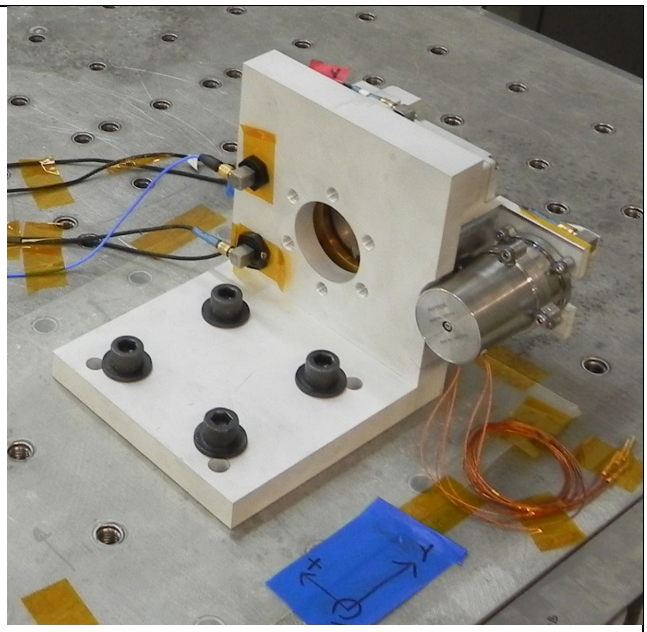

ii.) Rear side of the focus mechanism

Figure 32: Focus mechanism on the vibe table, prior to test, mounted to the L-bracket interface plate for environmental testing.

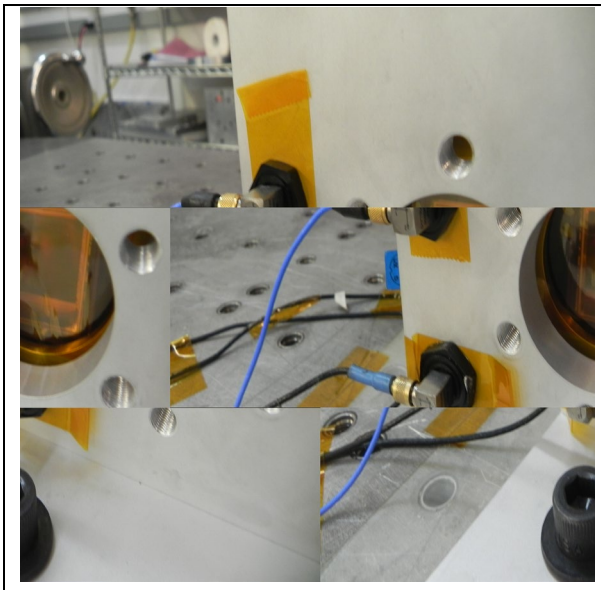

i.) Control locations

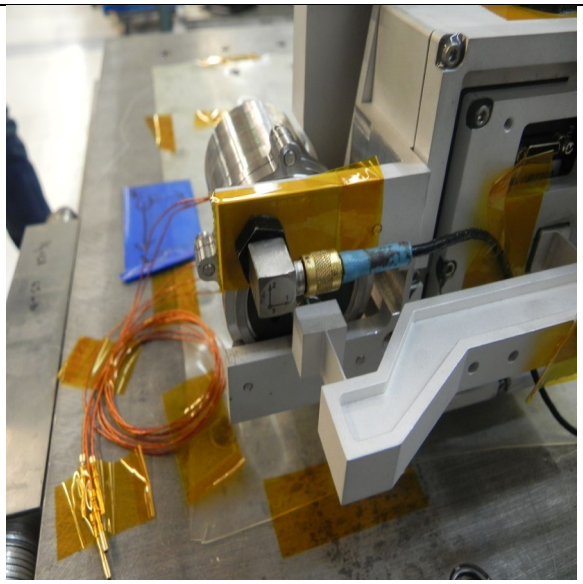

ii.) Motor body

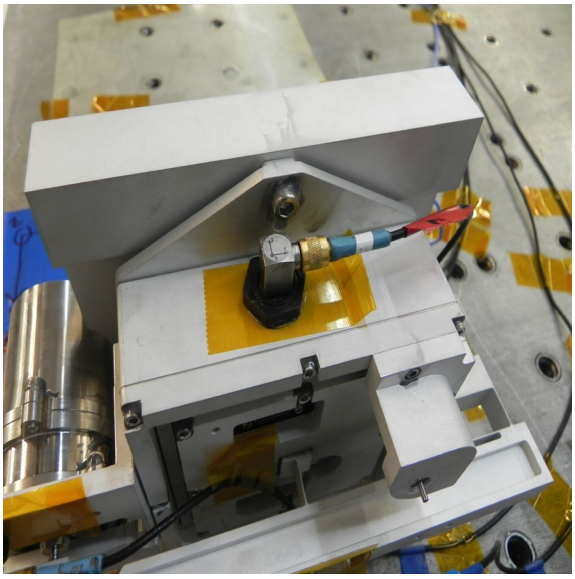

iii.) Camera housing

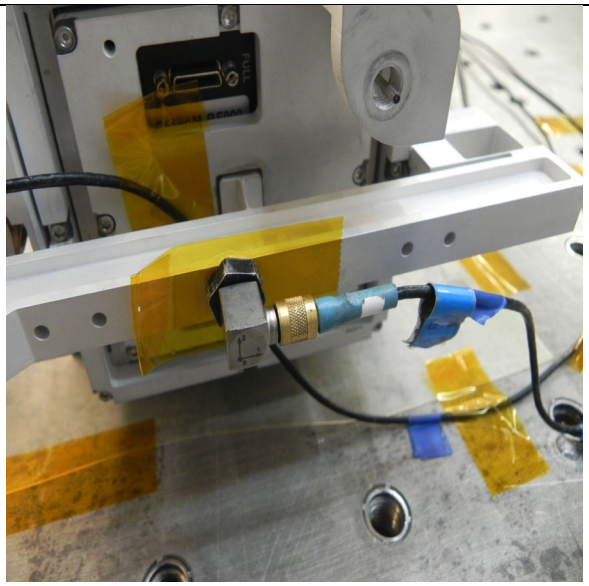

iv.) Flexure arm

Figure 33: Vibration test accelerometer placements, common for all three axes of tests.

2. Test Results

The following section presents the power spectral density (PSD) results for the focus mechanism in response to random vibration testing. First, the primary system response (i.e., the axis under excitation) is shown, followed by the before and after low-level random (LLR) sine sweeps. A brief analysis and discussion follow each test.

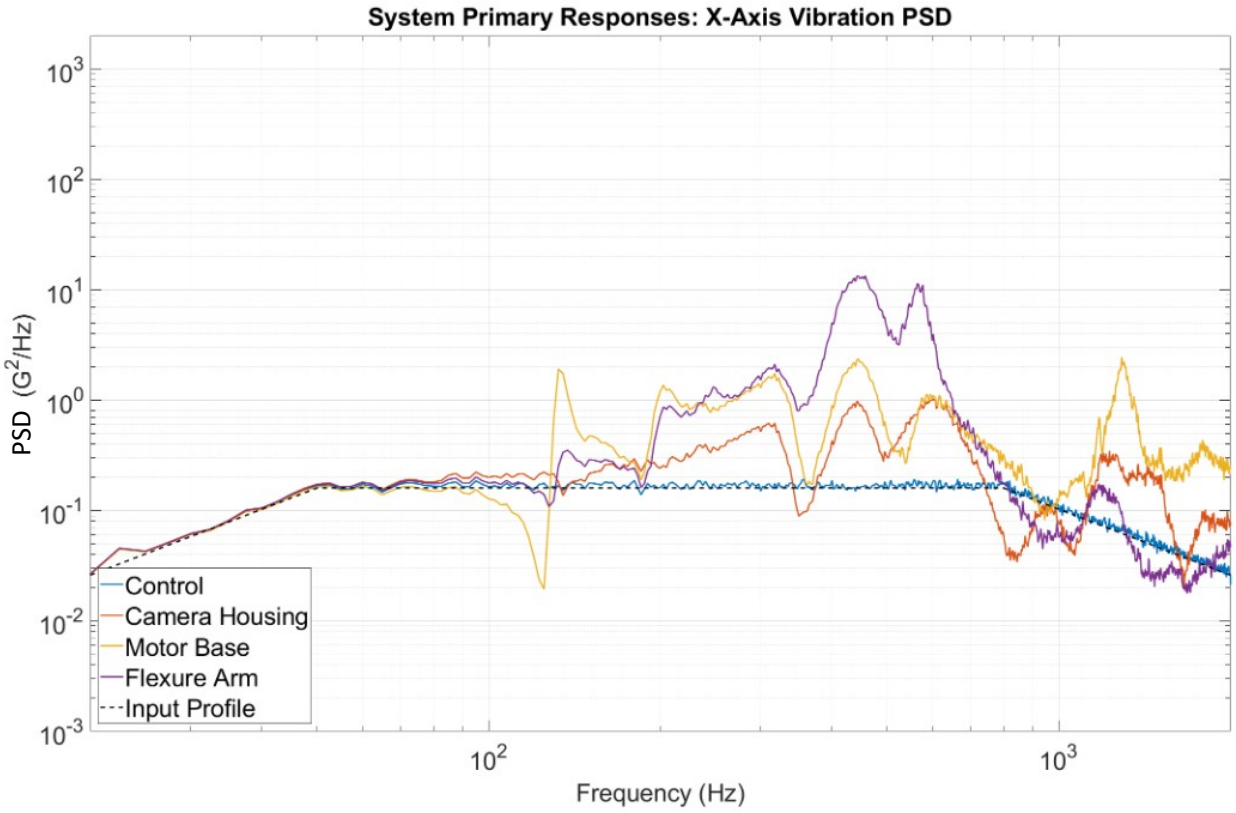

Figure 34: Principal axis response to X-axis random vibration excitation.

The control matched the input profile within a 3dB tolerance across the entire frequency range. Due to the long moment arm induced by the mounting configuration of the actuator, there is significant response above 100Hz, throughout the remainder of the test. The camera housing appears relatively well behaved throughout the frequency sweep. The flexure arm, as expected, showed the largest response at approximately 450-650Hz.

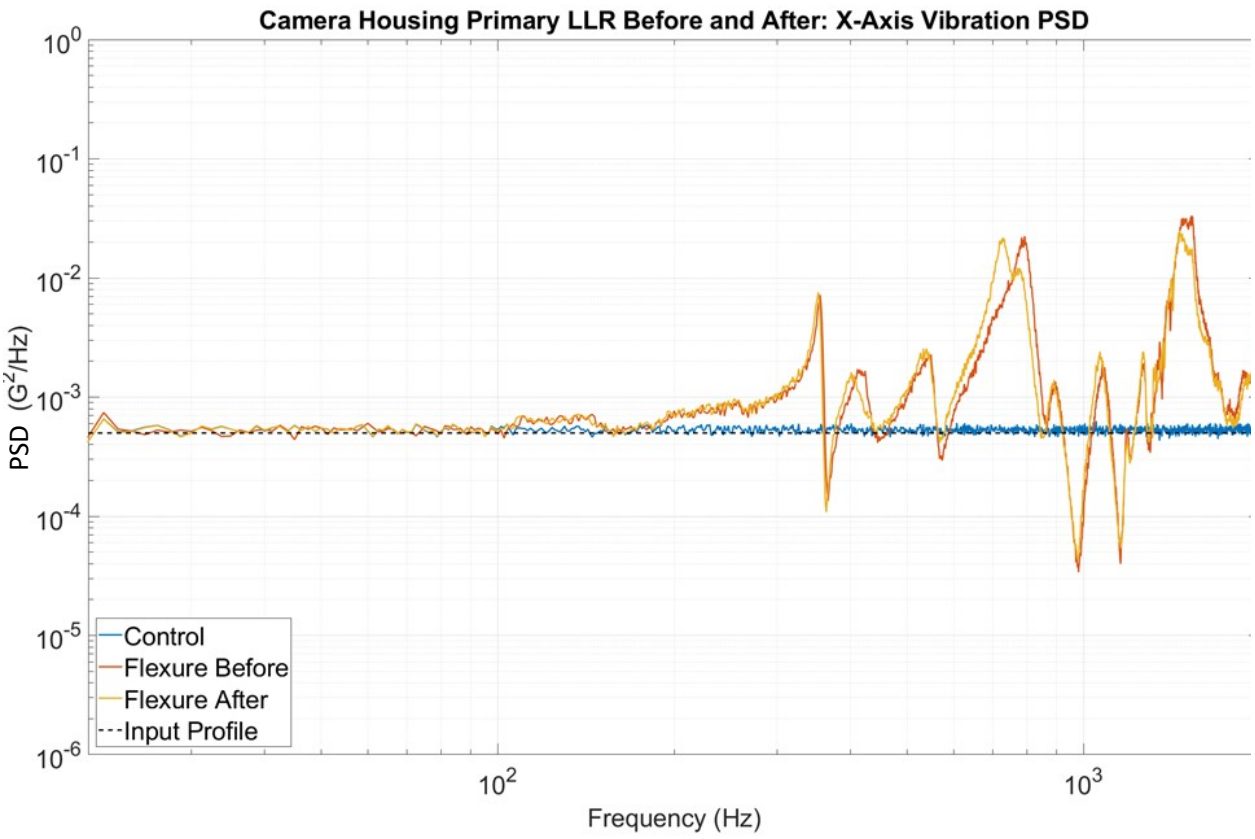

Figure 35: Comparison of low-level random sine sweep before and after X-axis vibration excitation.

The flexure arm is shown for three reasons: simplicity, it had the largest response, and it is the most sensitive component on the assembly. The LLR is well behaved before and after the primary excitation. There is a minor shift in frequency response at approximately 650Hz, which corresponds to the peak response in the vibration test.

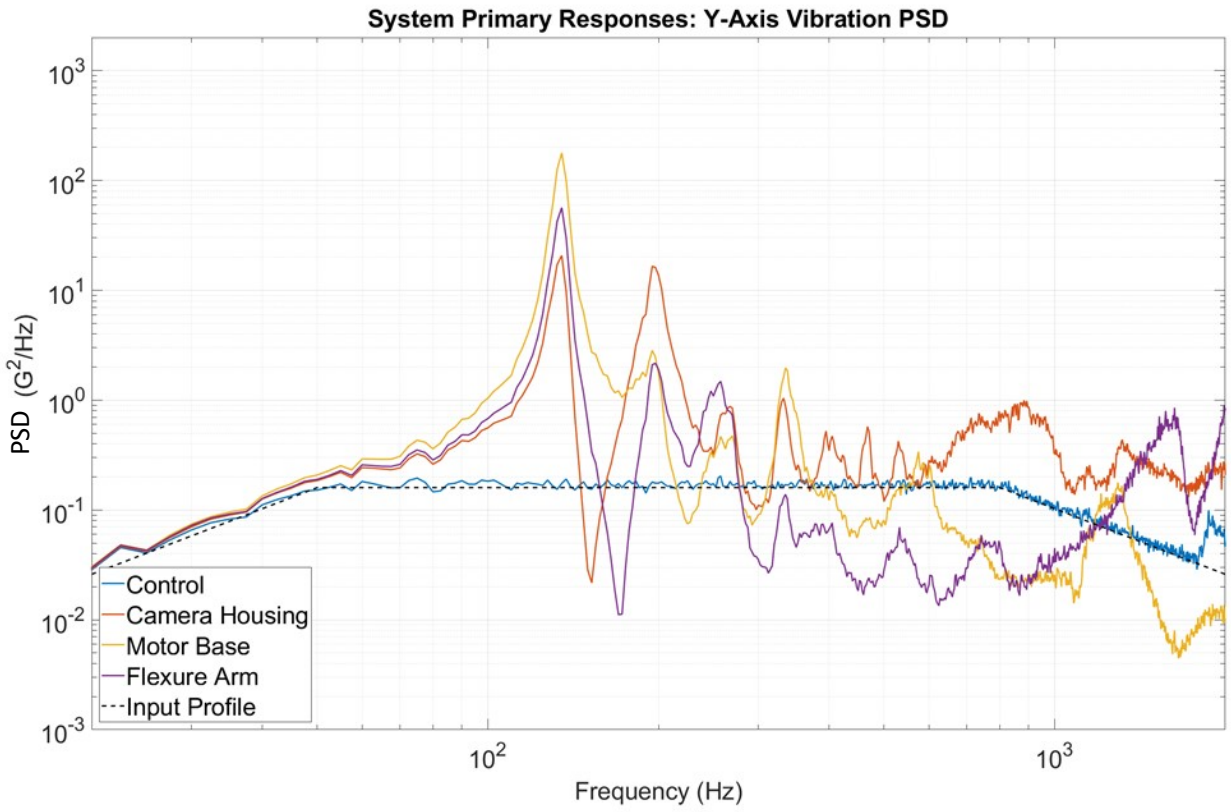

Figure 36: Principal axis response to Y-axis random vibration excitation.

The control matched the input profile to within the 3dB tolerance until the end of the sweep, at approximately 1,750Hz. Due to the deviation happening at the end of the frequency sweep, an abort was not called. All three measured components showed concerning resonances very low in the frequency sweep, at approximately 125Hz, and again at 200Hz. The camera housing showed a significant response beginning 650Hz.

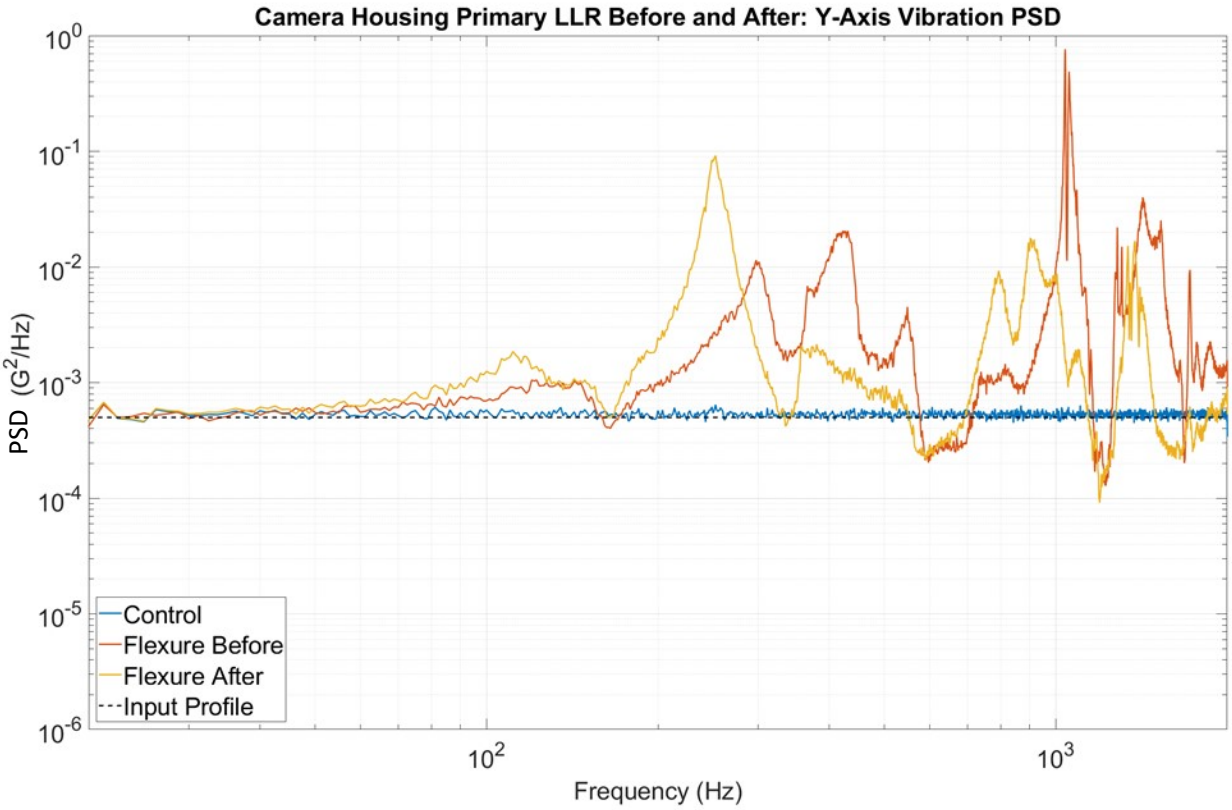

Figure 37: Comparison of low-level random sine sweep before and after X-axis vibration excitation.

For reasons stated previously, the flexure arm is the only component examined during LLR. There are significant and concerning shifts in response of the pre-and-post LLR. The first primary response, originally seen at 300Hz, shifted almost 50Hz and is now present at 250Hz. Though there have been significant shifts in the LLR behavior, it is not immediately clear whether or not this represents a mechanical settling or a buckling/failing of any components.

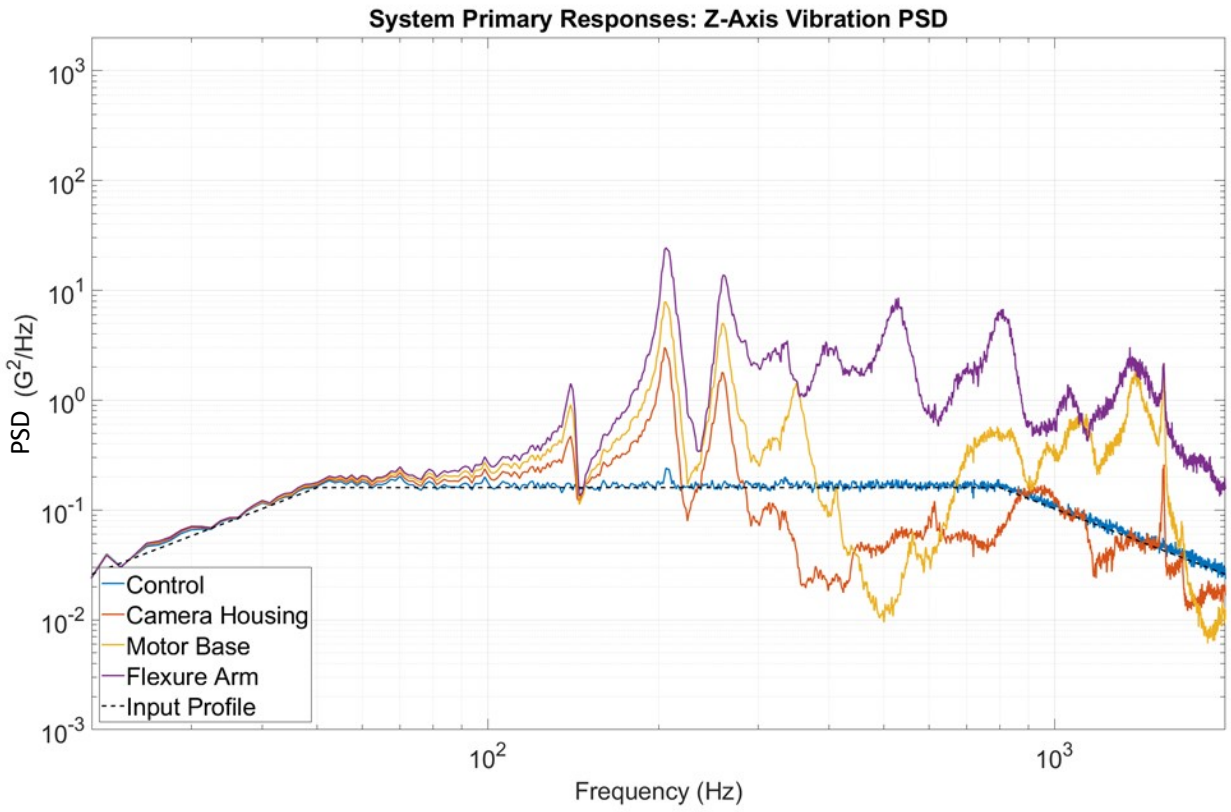

Figure 38: Principal axis response to Y-axis random vibration excitation.

The control matched the input profile within the 3dB tolerance across the frequency sweep. Surprisingly, the flexure arm showed the most significant (and sustained) response throughout the Z-axis excitation. This excitation is orthogonal to the long axis of the flexure, indicating that the response should be dampened. However, the above data shows the flexure arm was susceptible to excitation above 200Hz throughout the duration of the test. The camera housing had its primary response at approximately 200Hz, and again at 250Hz, then settled for the majority of the test. The motor base showed a similar response in the lower frequencies but began to show significant movement between 700 and 1,500Hz.

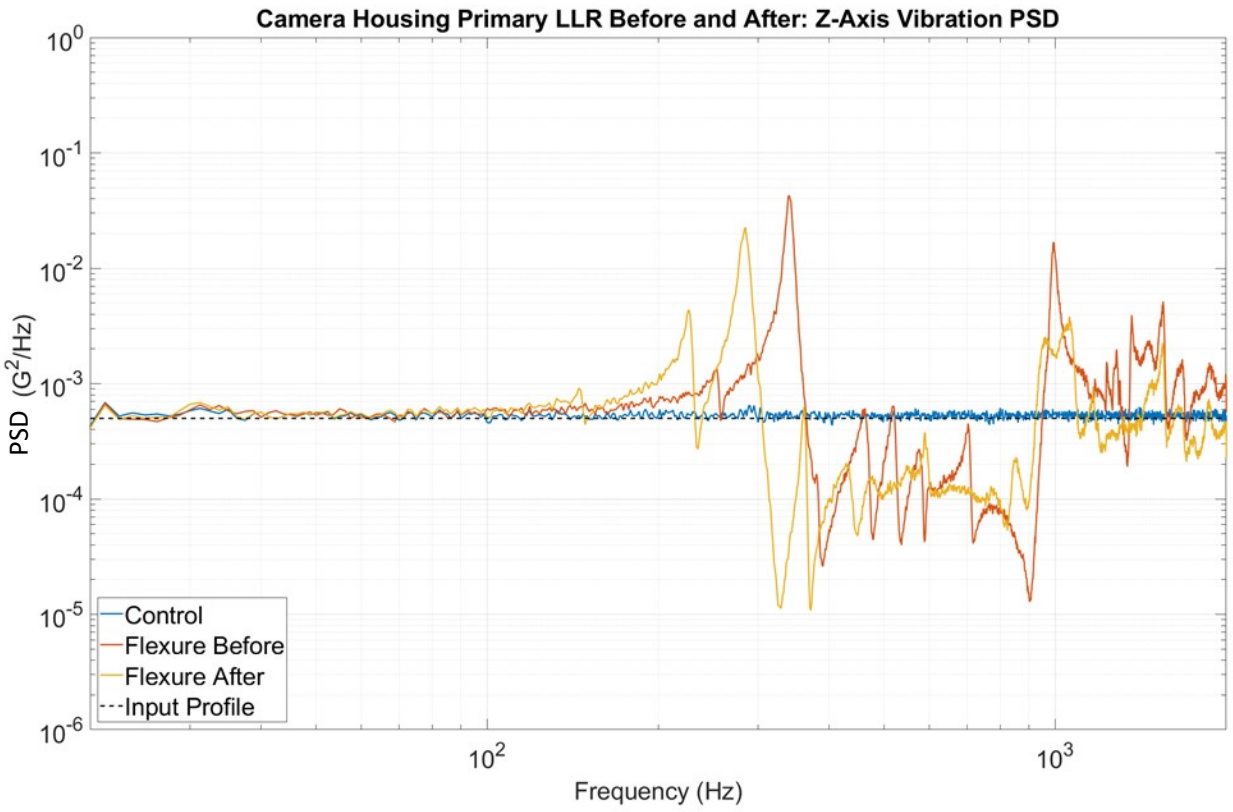

Figure 39: Comparison of low-level random sine sweep before and after Z-axis vibration excitation.

Similar to the Y-axis LLRs, the flexure shows a settling behavior of approximately 50Hz throughout the test. There is significant deviation between the behaviors of the pre-and-post tests seen from 400-2,000Hz.

The graphs shown in this section indicate there are concerning mechanical modes that are present in the system. However, due to the pass/fail success criteria of the vibration testing, these modes are not investigated further. Additional discussion about future work is found in Section V “Recommendations”.

B. Thermal

1. Test Setup

The following images show the focus mechanism in the thermal vacuum chamber prior to testing. Four k-type thermocouple channels were placed on the mechanism to monitor temperatures throughout the test. K-type thermocouples are well suited to the test range of -60 to 85C. Four thermocouples, and their locations, were chosen due to ease of accessibility.

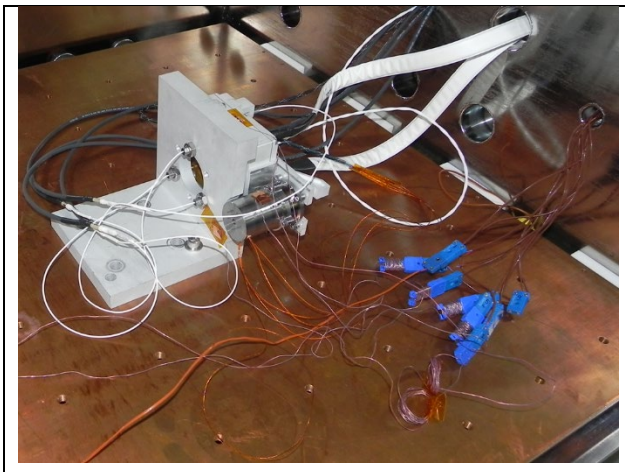

i.) Focus mechanism placed in the TVAC chamber

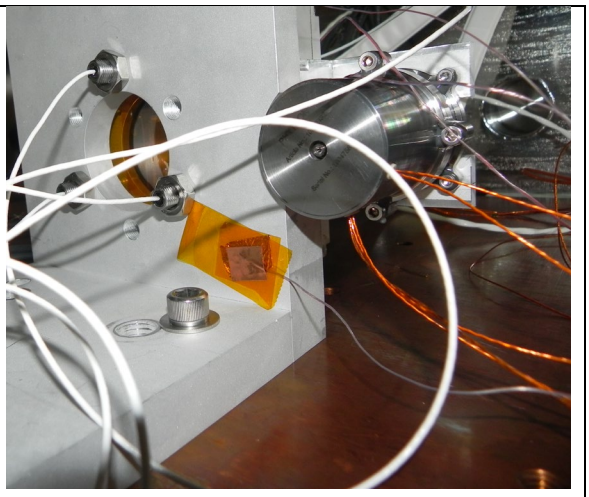

ii.) “Motor Body” and “Chamber” thermocouple placement.

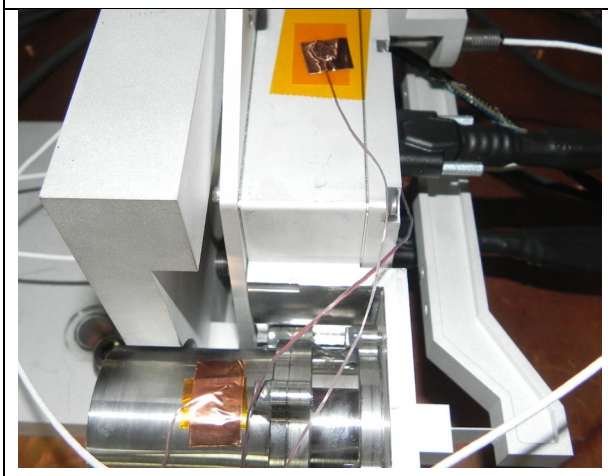

iii.) “tCamera” thermocouple placement

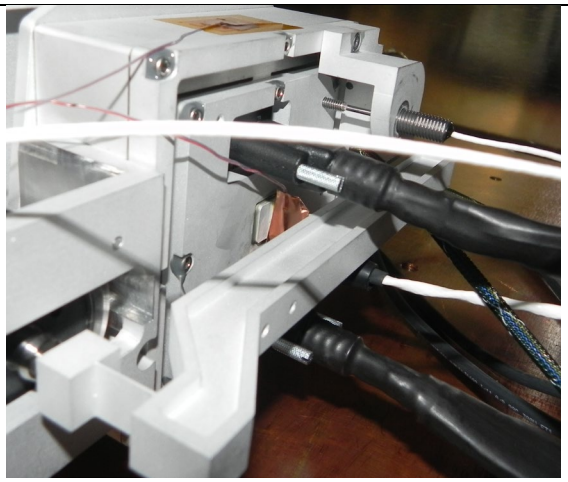

iv.) “bCamera” thermocouple placement

Figure 40: Focus mechanism loaded into thermal vacuum chamber prior to pump down. Included thermocouple placement and naming, as used on future graphs.

2. Test Results

The following shows the results from the TVAC test. In addition to pressure and temperature profiles, functional tests were taken during a hot and cold cycle. Due to the

extreme conditions of the TVAC chamber, it was not possible to include the calibration reference confocal sensor to accurately characterize the displacement characteristics of the actuator. However, the LVDT was included, and that data is included for reference. During each functional test, the actuator would be taken through its full 1,000 step range of motion, the image sensor would be turned on and have video streamed to the control PC. Because there was no optic or lens in front of the image sensor, no image was resolved. However, a light was flashed on and off, which could be discerned on the corresponding video stream. Because this test was used purely for proof-of-life, no video data was captured or saved. As long as a change (light or dark transitions) was observed, the electronics were deemed in an operable state.

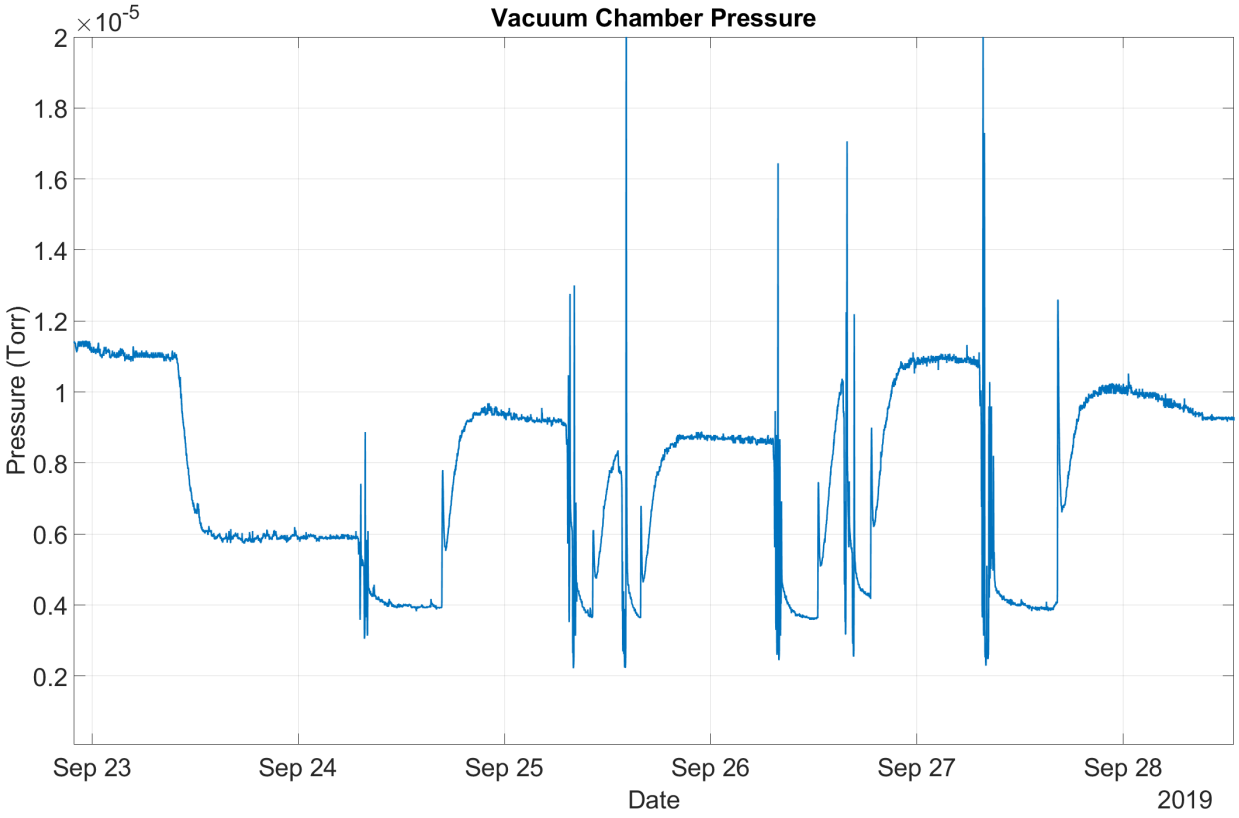

Figure 41: Pressure profile of TVAC chamber during testing.

The TVAC chamber achieved the 1E-5 Torr target pressure mid-day on Sep 23. At this time, the testing profile shown in the previous section began. Throughout the test, the pressure in the chamber stayed below the 1E-5 Torr target, with exception of single-point anomalies and a brief sustained period early on September 27. This corresponded to an elevated temperature of the camera, which likely caused additional volatiles to be outgassed.

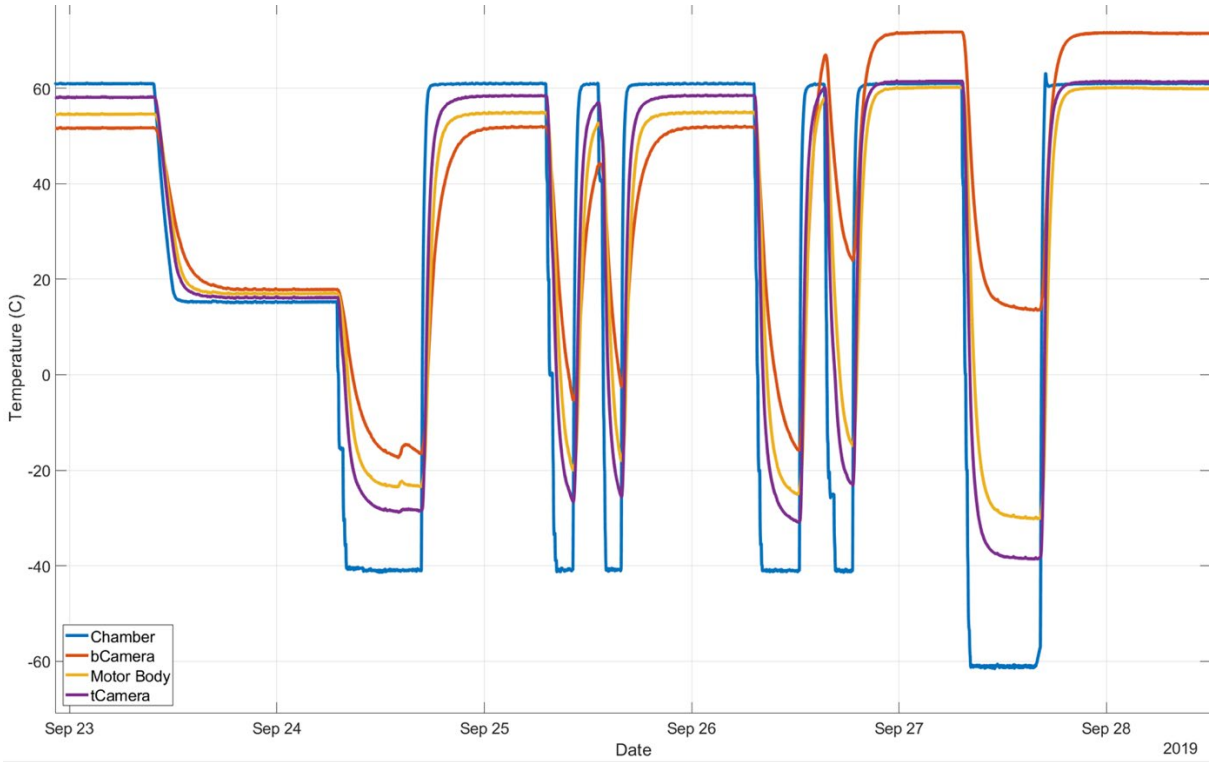

Figure 42: Temperature profile results for TVAC testing, once the chamber had hit 1E-5 Torr.

The chamber temperature matched the provided profile very closely (-40 to 60C dwells). Due to the lack of convection and limited conduction paths, the focus mechanism never reaches ambient chamber temperatures. Instead, the mechanism is always slightly warmer during cold soaks and slightly cooler during warm soaks.

The anomaly observed mid-day on Sep 24 is the cold functional test. The blip observed mid-day Sep 26 is the hot functional test. The sustained elevated temperature of bCamera (body of the camera) seen from mid-day throughout the rest of the test is because the camera was left on during these periods. This significantly impacted camera temperature but had little impact on the rest of the focus mechanism (top of the camera or the motor body during cold soaks. This was tested further, early on Sep 27, when the chamber was brought below the -40C target, all the way to -60C. Despite the additional 20C drop, the

motor body and top of camera remained consistent with -40C soak behavior. However, as can be seen mid-day Sep 27, the elevated temperature of the camera did provide enough additional energy for the motor body and top of the camera to achieve equal temperatures as the chamber.

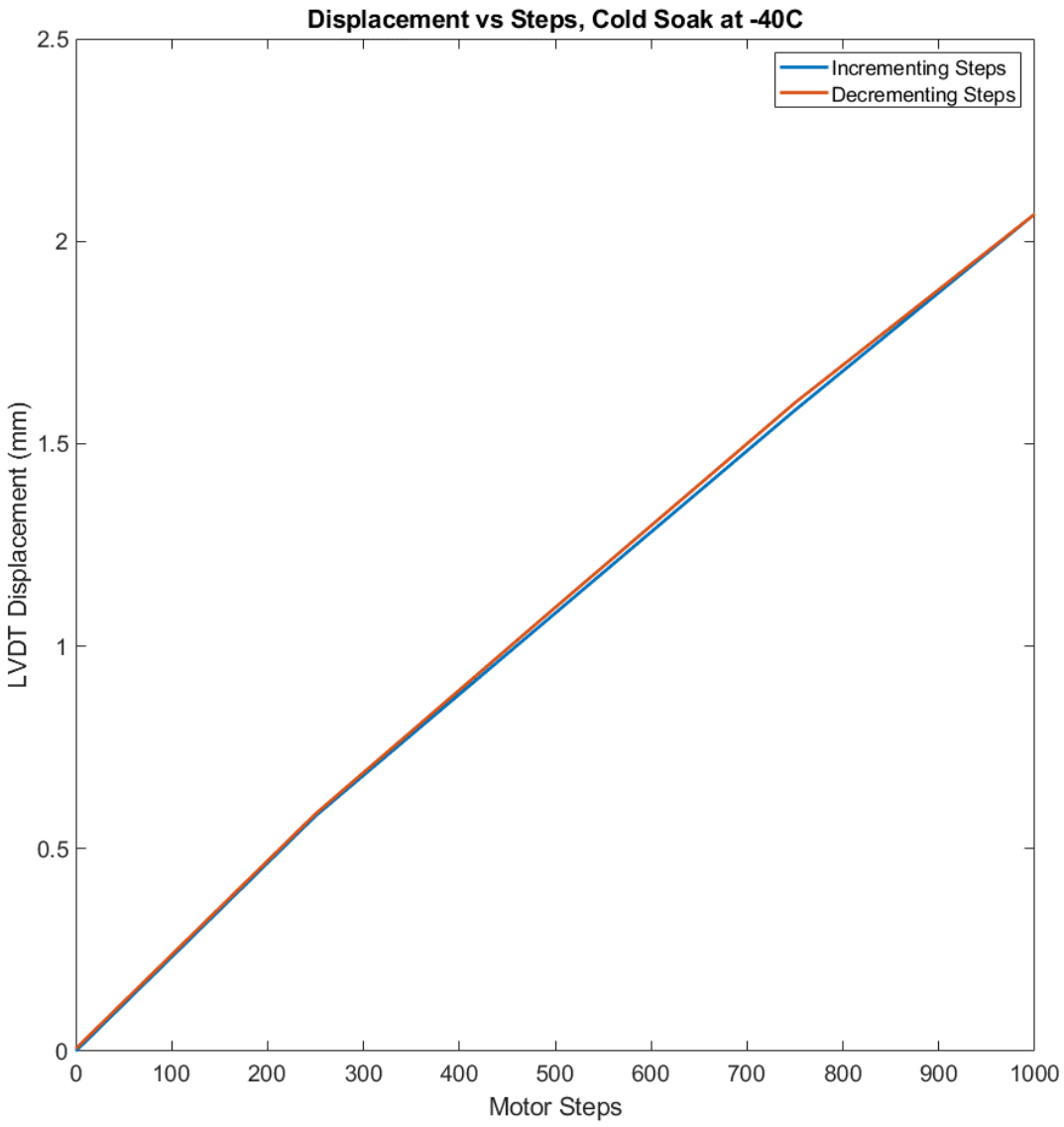

Figure 43: Focus mechanism displacement, as measured with the LVDT, during a -40C cold soak.

The above graph compares the displacement of the LVDT during the focus mechanisms actuation throughout its range of motion. Starting at 0 steps, the actuator was sent up to step 1000. Then, the actuator was commanded back down to step 0. The two lines compare the readout of the LVDTs, when converted to displacement using the calibration curves mentioned previously. Close alignment can be seen between these two measurements, indicating there was not a temperature dependency or other electrical malfunction at cold temperature. However, when this data is compared with the reference position data, there are significant deviations. The reference data showed step 500 corresponding to 1.22mm displacement (with high repeatability). The cold data shows step 500 corresponding to 1.096mm, a difference of 124um. This is a significant (and mission-impacting) difference. It is difficult to determine whether this difference is due to a temperature dependency of the system or mechanical differences induced by vibration testing. The reference data taken of the focus mechanism and actuator were taken at room temperature (approximately 23C). It was not in the scope of this thesis to determine future mitigation strategies for the observed deviation from reference data. Further discussion regarding the difference between environmental and reference data is held in Section V “Recommendations”.

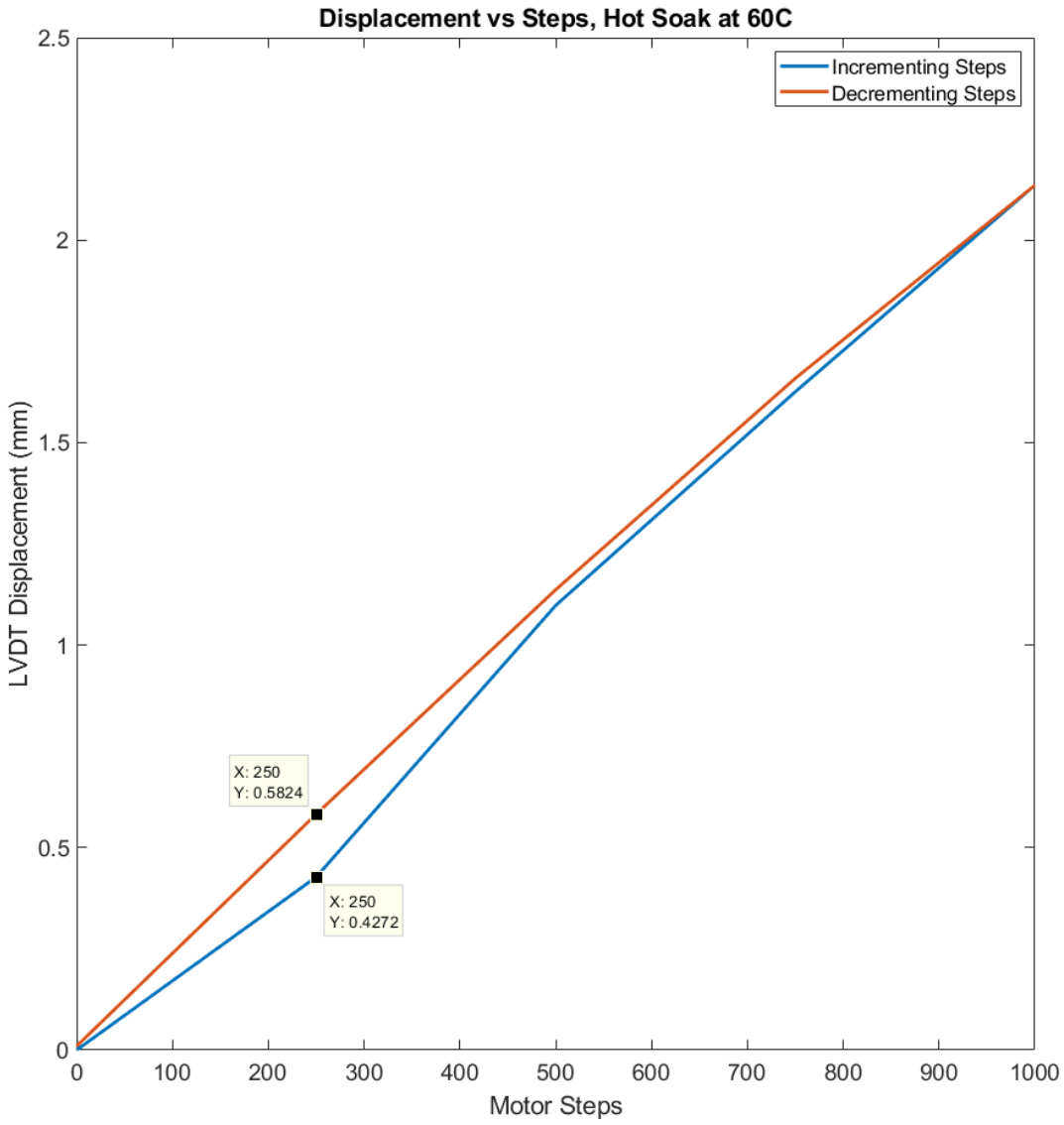

Figure 44: Focus mechanism displacement, as measured with the LVDT, during a 60C hot soak.

The data for the above graph was taken in the same manner as described previously. The hot soak displacement profile exhibited more concerning characteristics than the cold soak did. The incremental and decremental datasets varied significantly. As can be seen on Figure 36, the measured displacement at step 250 showed over a 150um difference. Additionally, step 500 corresponded to 1.098mm incrementing, 1.137mm decrementing,

and 1.22mm in the reference, corresponding to a maximum deviation of the datasets at 122um.

V. Recommendations

The first round of environmental testing was extremely enlightening, but the conclusions that could be drawn from the testing was limited due to a restrictive scope. The recommendations will be broken into three sections: Pre-Test, Test, and Post-Test recommendations. As the focus mechanism that was tested was simply the first engineering unit (EU), there are doubtless future units that will be designed, fabricated, characterized, and tested. For those who do not have this luxury (either due to budget or schedule constraints), closer attention should be paid throughout the entire design and test process.

Detailed pre- and post-test characterization were omitted in this effort, for both mechanical and electrical subsystems. For example, no dynamic finite element analysis was performed prior to vibration. Such analysis is useful in comparing predicted results with measured results. Detailed power measurements were not taken, and thus, no temperature dependency could be determined for the power consumption of the focus mechanism. Power consumption is of particular importance for space missions, as many times the space vehicle has very strict power budgets. Such omissions were justifiable, as the scope of the EU was intentionally limited. However, these oversights should be avoided to maximize the utility and effectiveness of environmental testing.

1. Pre-Test

While there was significant pre-test characterization done, as discussed in Section III.B, the final test results showed this stage to be significantly lacking. Specifically, either the actuator or the entire focus mechanism, as well as the LVDT, should have been characterized across its full temperature range prior to environmental testing. Due to three uncontrolled variables (temperature, pressure, and post-vibration performance), it was incredibly difficult to determine the source of any potential performance abnormalities during test. Characterizing the motor and electronics across their temperature range prior to integrated testing is particularly important, as electrical performance is known to have exceedingly strong temperature dependencies.

Additionally, a figure of merit should be established for the image sensor prior to testing. This is generally accomplished by read-noise and dark-current measurements. As it currently stood, besides a sign-of-life, there was no way to determine if the image sensor performance degraded due to vibration testing or through TVAC. Note: this sort of testing may be considered out-of-scope for any focus mechanism testing, as it is considered component-level with respect to the focus mechanism. By the time the sensor is integrated it should already be characterized. Whether testing is performed by the development team to establish an image sensor figure of merit, or if the test data is taken from a manufacturer reference, it is important to have prior to heading into environmental testing.

Finally, there should be significant mechanical modeling prior to environmental testing. A modal analysis was not performed, nor was any transient vibration analysis. This left uncertainty during the random vibration testing (and LLR) as to what would be the expected response. It was virtually impossible to determine any mechanical implications of the test, as there was no reference data heading into it. While this falls in line with the desired coarseness of the first engineering unit testing, such omissions should be avoided in future tests. For programs with limited budgets, multiple tests and engineering units may not be possible. In that case, it is especially important to have exhaustive reference data prior to testing.

2. Test

Closer attention should have been paid by a knowledgeable individual during the vibration analysis. Because there was no reference modal or transient finite element modeling, the best that could be determined was whether the vibration test caused visible failure. While sufficient for the spirit of testing in this thesis, the lack of detailed vibration analysis leaves much to be desired.

The vacuum testing was well executed and monitored. Due to the extended time of TVAC testing, a well-thought-out data acquisition plan should be developed. There is an inherent trade of between ease of analysis and fidelity. It is recommended that future work finds a better balance between these two. Additional thermocouples throughout the system would have provided superior data to aid with thermal characterization. The testing for this thesis were limited to four, due to ease of availability. A well-established test plan, prior to system integration, would have provided an opportunity for additional sensors.

3. Post-Test

There was no post-test analysis performed under this work. This is largely due to two reasons: additional design was conducted in parallel with the testing due to outside circumstances, and post-test analysis was out of scope for the initial work. The focus mechanism design changed more significantly than was originally thought, rendering any post-test analysis more or less an exercise in curiosity rather than utility. Even if the redesign had not been as extensive as it proved to be, post-test analysis was not the intent for this round. The motivation of this round of testing was to gain a preliminary understanding of the focus mechanisms capability in the extreme environments it would encounter on orbit, which was accomplished. As stated previously, to maximize utility out of a given round of testing, extensive pre- and post-test characterization of all subsystems should be performed.

Though a lack of post-test was appropriate for this effort, it leaves the majority of questions that were discovered during testing unanswered. It is standard practice to have a reference performance test (RPT). This serves as a baseline to return to after any significant event of the system. The RPT is designed to fully capture nominal performance of the system. For the focus mechanism, it would include average power statistics of the electronics, displacement characteristics of the actuator, and LVDT accuracy throughout the range of travel. For environmental testing, ideally, an RPT would be performed after each axis was excited during vibration, prior to heading into TVAC, and after TVAC.

If warranted, a detailed mechanical inspection of the focus mechanism after vibration would also be enlightening. The LLR throughout random vibration testing showed significant shifts. While these may not have been attributable to visual cues at an integrated level, they may become apparent at a component (or subassembly) level. Disassembling the focus mechanism and checking the tolerances on key mechanical components would show whether or not vibration testing caused a component-level failure.

VI. Conclusion

The impetus of this effort was to address a need in small satellite telescopes. In response, a single axis focus mechanism was designed, an engineering unit was built, and that unit underwent environmental testing. While the initial design is promising, the test results indicate there remains significant work to ensure adequate performance under extreme environments. It is important to note that the intent of this round of environmental testing was to gain some preliminary insight rather than to be exhaustive. By the success criteria, defined earlier in this thesis, the focus mechanism environmental testing was a success. It is the sincere hope of the author that the work will be continued and employed on a flight mission soon.

VII. References

Ailor, W., Womack, J., & Peterson, G. (2010). Effects of Space Debris on the Cost of Space Operations. *International Astronautical Congress*.

Alby, F., Lansard, E., & Michal, T. (1997). Collision of Cerise with Space Debris. *Second European Conference on Space Debris*, 589-596.

Bely, P. Y. (2003). *The Design and Construction of Large Optical Telescopes.* Springer-Verlag New York.

Bennion, K., & Thornton, M. (2010). Integrated Vehicle Thermal Management for Advanced Propulsion Technologies. *SAE 2010 World Congress.* Detroit: National Renewable Energy Laboratory.

Burgh, E., & Nordsieck, K. (2003). Prime Focus Imaging Spectrograph for the Southern African Large Telescope: optical design. *SPIE*.

Corporation, A. (1996). *Small Satellite Cost Model (SSCM).* El Sugundo: The Aerospace Corp.

Dinyari, R., Rim, S.-B., Huang, K., Catrysse, P., & Peumans, P. (2008). Curving monolithic silicon for nonplanar focal plane array applications. *Applied Physics Letter*, 92.

Dunn, M. (2016, 04 10). *NASA's planet-hunting Kepler Spacecraft in emergency mode*. Retrieved from My NBC 15: https://mynbc15.com/news/nation-world/nasas-planet-hunting-kepler-spacecraft-in-emergency-mode

Fiete, R. (2010). *Modeling the Imaging Chain of Digital Cameras.* SPIE.

Gilmore, D. G. (2002). *Spacecraft Thermal Control Handbook.* The Aerospace Press.

Girvin, H. (2007). *A Historical Appraisal of Mechanics.* Seattle: Girvin Press.

Gonzalez, R., & Woods, R. (2018). *Digital Image Processing.* Pearson.

(2019). *GSFC-STD-7000.* Greenbelt: NASA Goddard Space Flight Center.

Hastings, D., & Garrett, H. (1996). *Spacecraft-Environmental Interactions.* New York: Cambridge University Press.

International, G. (2017, 10 05). *Eni to Utilise Earth Observation Satellite Data and Services*. Retrieved from GIM International: https://www.gim-international.com/content/news/eni-to-utilise-earth-observation-satellite-data-and-services

Jahn, W., Ferrari, M., Hugot, E., Chambion, B., Moulin, G., Nikitushkina, L., . . . Gaeremynck, Y. (2016). Flexible focal plane arrays for UVOIR wide field instrumentation. *International Conference on Space Optics.* Biarritz.

James, M., Salton, A., & Downing, M. (2014). *Draft Environmental Assessment for Issuing an Experimental Permit to SpaceX for Operation of the Dragon Fly Vehicle at the McGregor Test Site.* Texas: Blue Ridge Research and Consulting LLC.

Kaufman, Y., & Justice, C. (1998). Potential Global Fire Monitoring from EOS-MODIS. *Journal of Geophysical Research-Atmospheres*, 32215-32238.

Labs, P. (2021). *Planet*. Retrieved from Planet: https://www.planet.com/company/

Larson, W. (2006). *Cost Effective Space Mission Operations.* McGraw Hill.

Larson, W., Kirkpatrick, D., Thomas, D., Sellers, J., & Verma, D. (2018). *Applied Space Systems Engineering.* CEI.

Madec, P.-Y. (2012). Overview of Deformable Mirror Technologies for Adaptive Optics and Astronomy. *Proceedings of SPIE - The International Society for Optical Engineering*, 8447.

MCC-1. (2021, February 20). Retrieved from phytron: https://www.phytron.eu/products/driver-controller/mcc-1/

NASA. (2003, 09 03). *Telescope History*. Retrieved from NASA Education: https://www.nasa.gov/audience/forstudents/9-12/features/telescope_feature_912.html

NASA. (2013). *General Environmental Verification Standards (GEVS) for GSFC Flight Programs and Proejcts.* NASA.

NASA. (2021). *Hubble Space Telescope*. Retrieved from NASA Missions: https://www.nasa.gov/mission_pages/hubble/main/index.html

NASA. (n.d.). *Arcsecond Space Telescope Enabling Research in Astrophysics (ASTERIA)*. Retrieved from Jet Propulsion Laboratory CubeSat: https://www.jpl.nasa.gov/cubesat/missions/asteria.php

NASA. (n.d.). *James Webb Space Telescope*. Retrieved from https://jwst.nasa.gov/

Park, W., Chang, S., & Lim, J. (2020). Development of Linear Astigmatism Free - Three Mirror System (LAF-TMS). *Publications of the Astronomical Society of the Pacific*.

Petruzella, F. (2016). *Electric Motors and Control Systems.* McGraw-Hill Education.

Planet. (2021). *Planet company*. Retrieved from https://www.planet.com/company/

Pugh, S. (1981). Concept selection: a method that works. *International Conference on Engineering Design*, (pp. 497-506). Rome.
Quintana, E. (2019, 08 01). Pandora: Multiwavelength Characterization of Exoplanets and Their Host Stars. NASA's Goddard Space Flight Center.
Schaller, R. (1997). Moore''s law: past, present, and future. *IEEE Spectrum*, 52-59.
Schlager, K. J. (1956). Systems engineering-key to modern development. *IRE Transactions on Engineering Management*, 64-66.
Sharkov, E. (2003). *Passive Microwave Remove Sensing of the Earth.* New York: Springer.
Werner, M. (2012). The Spitzer Space Telescope. *Optical Engineering*.
Wertz, J., Everett, D., & Puschell, J. (2011). *Space Mission Engineering: The New SMAD.* Microcosm Press.
Williams, K. (2013). *Latest Space Situational Awareness system heading to 1 SOPS*. Retrieved from Schriever Air Force Base: https://www.schriever.spaceforce.mil/News/Article-Display/Article/735935/latest-space-situational-awareness-system-heading-to-1-sops/
Williams, R. S. (2017). What's Next? [The end of Moore's law]. *Computing in Science & Engineering*, 7-13.
Wilson, R. (1999). *Reflecting Telescope Optics II.* Springer-Verlag Berlin Heidelberg.